eLife

Reviewed Preprint
v1 • May 29, 2025
Not revised

Reviewed Preprint
v2 • August 11, 2026
Revised by authors

SVEP1 enables efficient binding of Angiopoietin-2 to the TIE1 receptor, allowing receptor phosphorylation and downstream signaling

Katharina Uphoff[1,#], Melina Hußmann[1,2,#], Oliver Peters[3], Matthias Mörgelin[4], Fabian Metzen[5], Wolfgang MJ Obermann[5], J Fernando Bazan[6], Jörg Stetefeld[3] ✉, Manuel Koch[5] ✉, Stefan Schulte-Merker[1] ✉, Dörte Schulte-Ostermann[1] ✉

[1]Institute for Cardiovascular Organogenesis and Regeneration, Faculty of Medicine, University of Münster, Münster, Germany • [2]Division of Vascular Oncology and Metastasis, German Cancer Research Center, Heidelberg, Germany • [3]Department of Chemistry, University of Manitoba, Winnipeg, Canada • [4]Colzyx AB, Lund, Sweden • [5]Institute for Dental Research and Oral Musculoskeletal Biology, Faculty of Medicine and University Hospital Cologne, University of Cologne, Cologne, Germany • [6]ħ bioconsulting, llc, Stillwater, United States

For correspondence:
Jorg.Stetefeld@umanitoba.ca
manuel.Koch@uni-koeln.de
schultes@ukmuenster.de
d.schulte@uni-muenster.de

[#] Contributed equally

Competing interests: No competing interests declared

Funding: See page 28

Reviewing editor: Volker Dötsch, Goethe University Frankfurt, Germany

eLife Assessment

This manuscript focuses on developing a structural model of how the multidomain ECM protein SVEP1 enables Angiopoietin (ANG) binding to the orphan receptor TIE1, resulting in downstream receptor phosphorylation and signaling. This is an **important** study, based on **solid** data. The results will be of interest to scientists working in vascular biology and RTK signaling.

https://doi.org/10.7554/eLife.106338.2.sa3

Abstract

The molecular mechanisms that drive (lymph-)angiogenesis are crucial to understand diseases, such as lymphedema, that are caused due to malformations of the lymphatic vasculature. Recently, an interaction between the secreted protein Svep1, a key regulator in lymphangiogenesis, and the transmembrane receptor Tie1 was shown in zebrafish, human, and mice. Here, guided by *in silico* AlphaFold-multimer structure predictions of SVEP1 complexes, we assert with protein binding studies that the human CCP20 domain is the primary binding site for TIE1. We further demonstrate that SVEP1 mediates strong binding of ANG2 and TIE1, and that combined stimulation of hdLECs with SVEP1 and ANG2 leads to phosphorylation of TIE1. TIE1 activation by SVEP1 and ANG2 enables downstream signaling and, in turn, potentiates nuclear exclusion of FOXO1 and phosphorylation of AKT compared to SVEP1 or ANG2 alone. We present a model in which ANG1/2 dimers bind to both SVEP1 and TIE1, resulting in the recruitment of multiple TIE1 receptor molecules to a multimeric complex at the cell membrane, potentially amplifying its signaling capacity.

Introduction

Lymphatic vessels are closely associated with blood vessels, and malformations of the lymphatic vasculature lead to lymphedema, obesity, or chronic inflammatory diseases (Mäkinen et al. 2021; Petrova and Koh 2018; Sunil Kumar et al. 2025). Next to the well-described lymphatic VEGFC/VEGFR3 pathway (Hogan et al. 2009; Bos et al. 2011; Le Guen et al. 2014; Jeltsch et al. 2014; Roukens et al. 2015), it was shown that Sushi, von Willebrand factor type A, EGF, and pentraxin domain containing protein 1 (SVEP1), also referred to as Polydom, is another key player

in lymphangiogenesis (Karpanen et al. 2017; Morooka et al. 2017). Svep1 encodes a 3571 amino acid long extracellular matrix protein of different domains like von Willebrand factor type A domain (vWF), ephrin-receptor like domains, complex control protein (CCP) domains, and Hyalin repeats at the N-terminus. The C-terminus mainly consists of CCP and EGF domains. Svep1 is expressed in mesenchymal cells and functions non-cell-autonomously (Karpanen et al. 2017; Morooka et al. 2017). Only recently, it was discovered that SVEP1 binds to TIE1 (Hußmann et al. 2023; Sato-Nishiuchi et al. 2023), and we were able to provide *in vivo* evidence for the genetic interaction of *svep1* and *tie1* in zebrafish. Multiple phenotypic hallmarks of *svep1* mutants are phenocopied by *tie1*, but not *tie2* mutants, including (among others) a reduced number of parachordal lymphangioblasts (PLs) (Hußmann et al. 2023). Furthermore, a specific aspect of the facial lymphatics in zebrafish, the facial collecting lymphatic vessel (FCLV), develops in a *svep1* and *tie1* dependent, but *vegfc/vegfr3* and *tie2* independent manner (Hußmann et al. 2023).

The discovery of the novel molecular interaction between SVEP1 and TIE1 provided an invitation to further investigate how SVEP1 is linked to the already well-known ANG/TIE pathway. The ANG/TIE pathway triggers a signaling cascade, which is required for lymphatic and blood vessel development, and has a unique role in maintaining vascular stability. Two receptor tyrosine kinases (RTKs), tyrosine kinase with Ig and EGF domains (TIE1) and tyrosine endothelial kinase (TEK), also known as TIE2 (Dumont et al. 1993; Partanen et al. 1992), are activated through binding of angiopoietin ligands, including ANG1 and ANG2 (Davis et al. 1996; Maisonpierre et al. 1997). TIE1 and TIE2 exhibit a high degree of homology with a globular head domain consisting of three immunoglobulin-like (Ig) domains and three epidermal growth factor-like (EGF) modules and a short stalk formed by three fibronectin type III repeats, while the N-terminal two Ig domains of TIE2 harbor the angiopoietin binding site (Macdonald et al. 2006). TIE2 is considered the main player in angiogenesis, and its phosphorylation, triggered by ANG1 binding, induces downstream signaling via PI3K/Akt, which leads to inhibition of the transcription factor Forkhead box protein O1 (FOXO1) and repression of FOXO1 target genes -such as *Ang2* (Kim et al. 2000, Daly et al. 2004). Although TIE2 is needed for lymphangiogenesis in mouse embryos, with genetic deletions of *Tie2* in lymphatic vessels leading to subcutaneous edema (Souma et al. 2018), postnatal knock-out of *Tie2* in lymphatics of newborn mice only has an effect on lymphatic collecting vessels but not on cutaneous lymphatic capillaries (Korhonen et al. 2022; Shen et al. 2014). While ANG1 is an agonist of TIE2, ANG2 acts as a context-dependent weak agonist or antagonist for TIE2 that can inhibit the ANG1–TIE2 signaling axis (Saharinen, Eklund, and Alitalo 2017). TIE1 blocks the signaling cascade in a context dependent manner by forming heterodimers with TIE2 (Hansen et al. 2010; Marron et al. 2000; Saharinen et al. 2005; Savant et al. 2015; Seegar et al. 2010). On the other hand, *Tie1* deletion leads to defects in the lymphatic capillary network and primary lymphatic network remodeling (Korhonen et al. 2022; Shen et al. 2014).

In the present study we extend our understanding of SVEP1 binding to TIE1, utilizing *in silico*, *in vitro*, and *in vivo* techniques. We show that the binding of ANG2 to TIE1 is enhanced by SVEP1 leading to phosphorylation and downstream signaling of TIE1, thereby potentiating phosphorylation of AKT and nuclear exclusion of FOXO1. Our study helps to understand the interaction of important signaling pathway members involved in (lymph-)angiogenesis and provides a model that suggests local TIE1 multimerization through bridging functions of ANG1/2 in the presence of SVEP1.

Results

SVEP1 binds to the D1-D2 domain of TIE1

Previously, it had been shown that solid-phase binding assays of recombinant full-length murine SVEP1 protein display a significant binding of SVEP1 to TIE1, but not TIE2 (Sato-Nishiuchi et al. 2023). In a binary setup, i.e., without other proteins being present, we confirmed this observation utilizing surface plasmon resonance (SPR) technology and negative staining assays (Figure 1 C and D). Furthermore, and since AlphaFold2 (AF2) and AF3 are remarkably accurate predictors of evolutionarily conserved protein-protein interactions, we used their multimer

capabilities to search for significant contact points between the full-length, 3571 amino acid human SVEP1 chain and potential binding partners TIE1 and TIE2. As shown by the comparative PAE (Predicted Aligned Error, a prediction quality and model confidence metric) plots of the full-length SVEP1 matches with TIE1 and TIE2 (Figure 1A, B), we observe clustering between the headpiece or N-terminal D1-D4 domains of TIE1 and the CCP19-21 stretch of SVEP1, in line with the results of Sato-Nishiuchi et al. (2023) which center on the CCP20 domain of murine SVEP1 for TIE1 capture. D1 and D2 refer to the two N-terminal Ig domains, D3 refers to the three EGF domains, and D4 to the third Ig domain of TIE1 or TIE2. By contrast, the PAE plot for the D1-D4 segment of TIE2 fails to show an equivalent clustering with the CCP19-21 stretch of full-length SVEP1. The more focused interrogation and modeling of equivalent N-terminal TIE1 and TIE2 ecto-domains with the isolated CCP19-CCP21 domain fragment of SVEP1 (using AF2.3 multimer) affirms the interaction interface of SVEP1 to TIE1, positioning the groove between the side-by-side packed Ig-like D1-D2 domains of TIE1 in close contact with the CCP20 domain of SVEP1, revealing an interaction surface area of 851,5 $Å^2$ marked by 8 H-bonds and 2 salt bridges by PDBePISA analysis (Supplementary Figure 1.1). The SVEP1-binding domains of TIE1 are buttressed by a Cys-rich D3 domain that links to an outstretched D4 Ig module that further connects to a linear array of D5-D7 FnIII domains N-terminal to the hydrophobic TM helix. Key regions and contacts illustrating salt bridges, hydrogen bond network surface, electrostatic potential representation and hydrophobicity surface representations are shown in supplementary Figure 1.2. In this closer examination of molecular fragments of TIE2 and SVEP1, AF2.3 multimer scores the interface lower in both ipTM (interface predicted template modelling) and actifpTM (actual interface predicted template modelling) metrics (Supplementary Figure 1.1) and qualitatively weaker binding to the CCP19-21 fragment of SVEP1. The resulting SVEP1-TIE2 model shows the D1 and D2 domains of TIE2 perched between the CCP20 and CCP21 domains of SVEP1 (Figure 1B). While PDBePISA analysis shows a similar interface surface area of 889.4 $Å^2$, only 2 H-bonds and 1 salt bridges are observed, suggesting a weaker interface. To verify the modelling results, we performed SPR assays with a 70 kDa version of the SVEP1 protein that contains the CCP20 domain (Figure 1C). We observed interaction of SVEP1 with TIE1, but not with TIE2 in the absence of other proteins. Furthermore, utilizing negative staining and transmission electron microscopy, we were able to directly visualize the attachment of SVEP1 and TIE1 (Figure 1D). As shown in supplementary Figure 1.2, modelling of SVEP1 and TIE1 suggested P202 and L203 of TIE1 as a key contact region. Accordingly, a TIE1 (P202L-L203F) mutant was not able to bind to SVEP1 (Supplementary Figure 1.3B). In addition and in agreement with a previous study, a SVEP1 (E2568A-G2569A) mutant in which two crucial amino acids in the CCP20 domain are exchanged could not bind to TIE1 (Supplementary Figure 1.3A).

ANG1/2 strengthens the binding capacity of SVEP1 and TIE1

Murine SVEP1 binds ANG1 and ANG2 *in vitro* (Morooka et al. 2017), and it has long been known that ANG1 and ANG2 bind to TIE2 (Davis et al. 1996; Maisonpierre et al. 1997). Both AF2 and AF3 multimer models effectively capture TIE1 in a complex with SVEP1 CCP20, so we next explored how the addition of ANG1/2 would affect this assembly (Figure 2A). The affinity of TIE1 for SVEP1 is significantly increased by the simultaneous binding of the C-terminal domains of ANG1 or ANG2 to the CCP20 module, as suggested by the increased PAE and ipTM scores, which improve on the binary coupling of just TIE1 to SVEP1 (Supplementary Figure 2.1). By contrast (not shown), TIE2 was not predicted to stably co-bind with ANG1/2 to CCP19-CCP21 of SVEP1 because the weaker binding of TIE2 with CCP19-CCP21 of SVEP1 fails to nucleate the formation of a ternary complex. The conformation of the TIE1-ANG1/2 heteromers in the SVEP1-bound pose resembles the solved X-ray structures of TIE2 bound to either ANG1 or ANG2 (PDB codes 4K0V and 2GY7, respectively, in the absence of any experimental TIE1-ANG complexes) (Supplementary Figure 2.1), and furthermore, the equivalent ANG1/2-binding epitopes in TIE1 are not blocked by SVEP1 binding. Whereas the two TIE2 X-ray complexes show a buried surface area of ~1200 $Å^2$ (with 2 H-bonds and 2 salt bridges) against ANG1/2, the addition of the SVEP1-TIE1 contact produces a combined ~1800 $Å^2$ interaction surface area as well as new contacts between SVEP1-

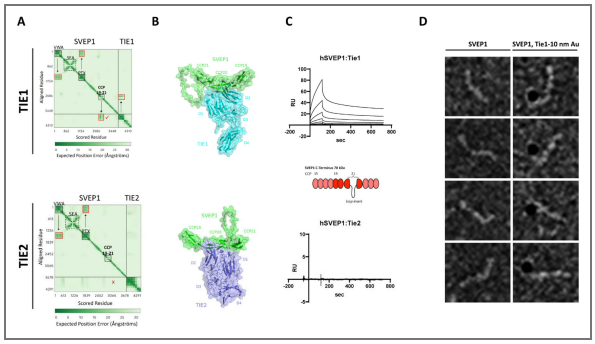

Figure 1. The CCP20 domain of SVEP1 contacts the D1-D2 headpiece domains of TIE1.

(**A**) Comparative PAE plots of full-length SVEP1 and the TIE1 ectodomain displays a primary binding site for TIE1 (domains D1-D2) by AF3-multimer modeling, that localizes to the CCP19-21 stretch, notably encompassing CCP20.. The PAE plot for full-length SVEP1 and the TIE2 ectodomain does not show an equivalent prediction for the same CCP19-21 region. Labelled SVEP1 domains: PTX (Pentraxin), SEA (sperm protein, enterokinase and agrin) module, VWA (von Willebrand factor type A), statistics flSVEP1-ectoTIE1 pLDDT = 66.1; pTM = 0.34; ipTM = 0.48; statistics flSVEP1-ectoTIE2 pLDDT = 0.68, ipTM = 0.28, pTM = 0.34 (**B**) A discrete AF2.3 model of TIE1 bound to CCP19-21 shows that the Ig-like D1-D2 headpiece domains of TIE1 (linked by a Cys-rich D3 to an 'open' or flared-out D4 Ig module) are in contact with CCP20. By contrast, the AF2.3 model of TIE2's N-terminal domains is more loosely perched between the CCP20 and CCP21 domains with a qualitatively lower affinity due to reduced sidechain contacts. (**C**) Quantitative analysis of TIE1-SVEP1 interaction using SPR assays. In the absence of other proteins, a 70kD version of SVEP1 (CCP15-CCP24, amino acids: 2261-2890; depicted in diagram fashion) containing the CCP20 domain binds TIE1 (K_D = 62.5 nM), but does not bind TIE2. (**D**) Negative staining shows binding of human C-term SVEP1-Strep II (reaching from CCP15 to the C-Term) and TIE1, labelled with 10nm Au. PAE: Predicted aligned error; AF3: AlphaFold 3; CCP: complement control protein (sushi repeats).

ANG1 and SVEP1-ANG2 (3 H-bonds and 1 H-bond, respectively) (Supplementary Figure 2.1). For this reason, SVEP1's CCP20 module acts as a binding partner for TIE1, but not TIE2, when interacting with ANG1/2.

ELISA assays verified the model prediction as the presence of either ANG1 or ANG2 led to a lower KD value (SVEP1, TIE1 (KD = 146,9) vs. SVEP1, TIE1, ANG1 (KD = 82,4); SVEP1, TIE1 (KD = 189) vs. SVEP1, TIE1, ANG2 (KD = 55,6)), reflecting a higher affinity (Figure 2B). Furthermore, co-transfection of either ANG1 or ANG2 together with TIE1 and subsequent immunoprecipitation of SVEP1 bound to beads verified the model prediction (Figure 2C). Whereas SVEP1 levels in all samples were similar, the level of TIE1 bound to SVEP1 significantly increased when ANG1/2 was present in the lysate. TIE1 co-transfected with ANG1 led to a slight, but not significant, increase in TIE1 levels. However, after transfection of TIE1, ANG1 and ANG2 levels are decreased in the total lysate. Thus, we were not able to detect ANG1 or ANG2 after immunoprecipitation.

Furthermore, negative staining shows binding of TIE1 and ANG1/2 to SVEP1 (Supplementary figure2.2)

Stimulation by SVEP1 and ANG1/ANG2 leads to phosphorylation of TIE1, nuclear exclusion of FOXO1, and phosphorylation of AKT

In previous studies, phosphorylation of TIE1 could not be detected after stimulation of cells with SVEP1 (Sato-Nishiuchi et al. 2023) or ANG2 (Saharinen et al. 2005) only, whereas stimulation of EA.hy926 immortalized hybrid HUVECs with ANG1, ANG4, and COMP-ANG1 leads to phosphorylation of TIE1 (Saharinen et al. 2005). Our aim was to test whether cooperative binding of SVEP1 and angiopoietins to TIE1 can lead to TIE1 phosphorylation, where SVEP1 constitutes the connecting link between TIE1 and ANG2. Indeed, after stimulation of hdLECs with both SVEP1 and ANG2, robust phosphorylation of TIE1 at residue pY^{1007} was detected (Figure 3A and D). Also, stimulation with SVEP1 alone has a slight effect on the phosphorylation of TIE1, possibly because hdLECs express ANG2 (Korhonen et al. 2022). To further test whether SVEP1-ANG2 stimulation leads to downstream signaling, we analyzed pAKT levels. Stimulation with either ANG2 or SVEP1 led to phosphorylation of AKT, which was amplified by simultaneous stimulation with ANG2 and SVEP1. The effect of SVEP1 stimulation on AKT signaling could be blocked by an ANG2 blocking antibody, suggesting that SVEP1 does not induce signaling on its own, but enables signaling of ANG2 (Figure 3B and E). Knock-down of either TIE1 or TIE2 could reduce activation of pAKT, leading to the assumption that both TIE1 and TIE2 are necessary for the phosphorylation of AKT after SVEP1-ANG2 stimulation and thus downstream signaling. Furthermore, we analyzed FOXO1 nuclear exclusion, a downstream event of the PI3K/AKT pathway, by stimulating hdLECs with either ANG2 or SVEP1, or both proteins in combination, and testing for nuclear versus cytoplasmic FOXO1 ratios. It has already been shown that SVEP1 activates the PI3K-Akt signaling pathway *in vitro*, with nuclear exclusion of FOXO1 (Sato-Nishiuchi et al. 2023). We observed enhanced nuclear exclusion of FOXO1 in hdLECs stimulated with combined SVEP1 and ANG2 compared to ANG2 or SVEP1 alone (Figure 3C), indicating that ANG2 potentiates the activation of PI3K-Akt and thus inactivates FOXO1. ANG2 by itself had a comparable effect on the FOXO1 inactivation as SVEP1, with both proteins showing a significant effect (Figure 3F).

SVEP1, TIE1, and ANG1/2 are predicted to form higher-order complexes

The results show that SVEP1 together with ANG2 lead to phosphorylation of TIE1, which then activates the PI3K-AKT signaling pathway, leading to nuclear exclusion of FOXO1. Previous studies have demonstrated the importance of TIE2 receptor clustering and its impact on downstream signaling (Kim et al. 2009). To explore the ability of the SVEP1, TIE1, and ANG1/2 complexes to form higher order assemblies, we utilized AF3 to model a 2:2:2 complex. AF3 predicted that the previously modelled ternary complexes (Figure 2A) are incorporated into a larger assembly of dimerized TIE1 receptors (Figure 4A). In the presence of ANG1/2 and SVEP1, AF3 predicts that

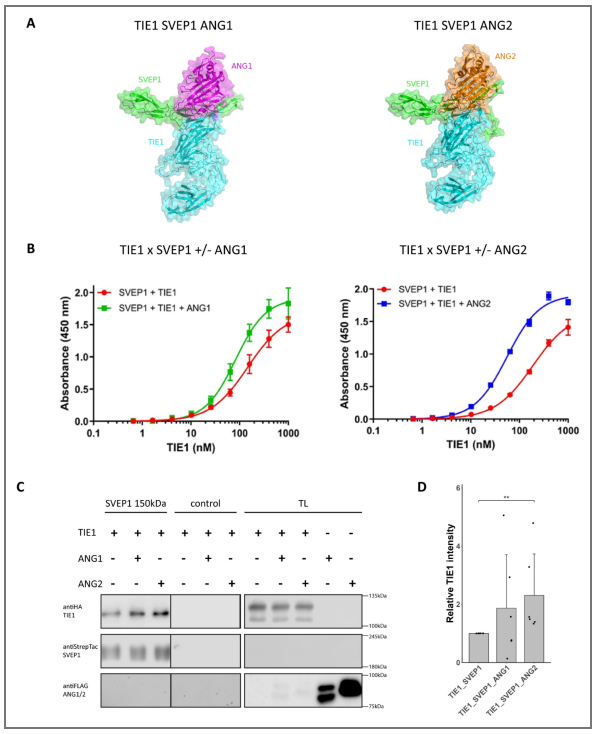

Figure 2. ANG1/2 strengthens the binding capacity of SVEP1 and TIE1.

(**A**) AF2.3-modeling of the SVEP1 CCP19-21 domain and TIE1 together with ANG1/2. The affinity of TIE1 for SVEP1 is considerably heightened by the co-binding of ANG1 or ANG2 C-terminal domains to the CCP20 module. (**B**) The Interaction between the complete C-terminal SVEP1 (spanning from the EGF1 domain to C-terminus) and the ectodomain of TIE1 was analyzed by ELISA binding assays. SVEP1 proteins were immobilized on 96 well plastic plates and overlayed with serial dilutions of TIE1 fused to an ALFA-tag, in the absence or presence of equal amounts of ANG2 as indicated. Bound TIE1 proteins were detected by HRP conjugated anti-ALFA-tag nanobody. ANG2 binding was detected using an HRP conjugated anti-Biotin antibody against the biotinylated protein. KD values are lower in the presence of ANG1 (K_D=82,4) or ANG2 (K_D=55,6), reflecting a higher affinity than SVEP1 and TIE1 in the absence of angiopoietins (K_D=189,0). (**C**) Co-immunoprecipitation of human TIE1 co-transfected with either human ANG1 or ANG2 in 293T HEK cells. Human SVEP1-Strep II (a 150 kDa version reaching from CCP15 to the C-Term) was immunoprecipitated, and associated TIE1 and ANG1/2 were detected via Western blot analysis. (**D**) Quantification of the TIE1 levels with SVEP1 levels as a reference confirmed a significant increase in binding affinity of SVEP1 and TIE1 together with ANG2 (**p.adj = 0.008; Mann–Whitney U test; Values are presented as means ± SD; individual data points for each experiment). TL, total lysate.

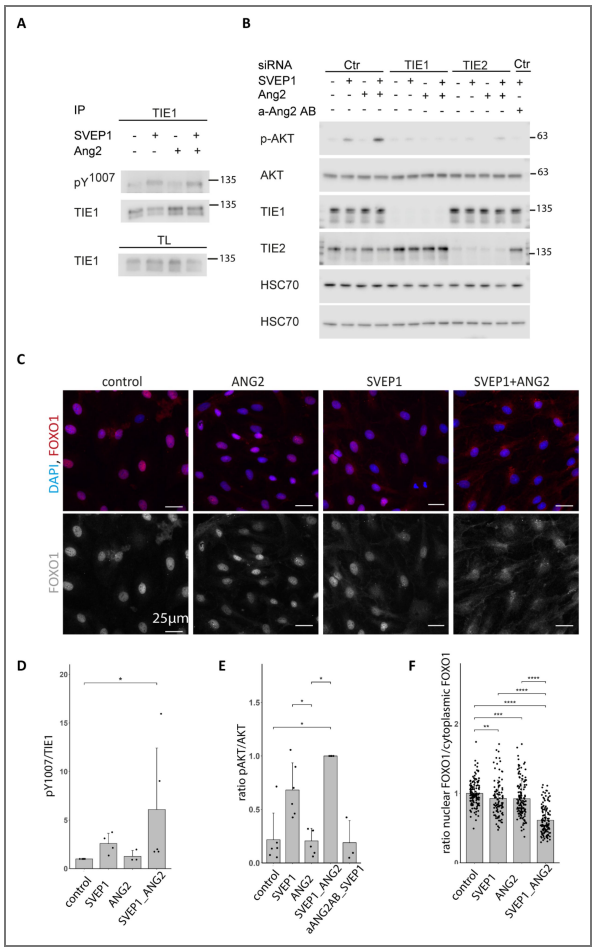

Figure 3. Simultaneous stimulation of LECs with SVEP1 and ANG2 leads to phosphorylation of TIE1 and AKT as well as nuclear exclusion of FOXO1 *in vitro*.

(**A**) Western blot analysis of TIE1 phosphorylation at Y^{1007} residue in SVEP1 and/or ANG2 stimulated LECs after immunoprecipitation of TIE1. TIE1 is phosphorylated after simultaneous stimulation with SVEP1 and ANG2. The antibody anti–phospho-TIE2 (pY992, AF2720 R&D Systems) detects both, TIE1 phosphorylation (at Y1007 residue) and TIE2 phosphorylation (at Y992 residue), but can be distinguished by size (Brouillard et al. 2024). (**B**) Western blot analysis of p-AKT and AKT in the cell lysate of SVEP1 and ANG2 stimulated LECs. Knock-down of either TIE1 or TIE2 leads to reduced induction of phosphorylation of AKT by SVEP1-ANG2 (**C**) FOXO1 (red) and DAPI (blue) staining of LECs stimulated with only SVEP1 or ANG2, or in combination. FOXO1 staining is restricted to the nucleus of unstimulated (control) LECs, whereas in cells stimulated with SVEP1 and ANG2 together FOXO1 is in the cytoplasm. (**D**) Quantification of the pTIE1/total TIE1 ratios shown in A. (N = 5; *p adj = 0,045; Mann–Whitney U test; Values are presented as means ± SD) (**E**) Quantification of the pAKT/total AKT ratios shown in B. Values are presented as means ± SD, N = 3/6; Mann–Whitney U test; Control vs. ANG2_SVEP1 p.adj = 0.028 *; SVEP1 vs. ANG2 p.adj = 0.022 *; ANG2 vs. ANG2_SVEP1 p.adj = 0.028 *; ANG2_SVEP1 vs. aANG2AB_SVEP1 p.adj = 0.091. (**F**) The ratio of nuclear FOXO1/cytoplasmic FOXO1 decreases after stimulation with either ANG2 or SVEP1. Stimulation of LECs with simultaneous SVEP1 and ANG2 leads to a further reduction of the nuclear FOXO1/cytoplasmic FOXO1 ratio. Each datapoint represents the mean value per image of the ratio of nuclear to cytoplasmic FOXO1 per cell (Mann–Whitney U test; Values are presented as means ± SD; N=4).

TIE1 dimerization is mediated by Fn3-Fn2' contact as well as crossing over at the D3 and D4 domains (Figure 4B) with acceptable confidence metrics (Supplementary Figure 4 and Supplementary Figure 4.1). In addition to TIE1 dimerization, both ANG1 and ANG2 dimerize via a N-terminal coiled-coil domain and can multimerize into larger assemblies by interchain disulfide bonds (Kim et al. 2005). ANG1/2 multimerization is crucial for proper TIE2 activation (Kim et al. 2009) and ANG1/2 together with SVEP1 may have a similar effect with TIE1, clustering TIE1 receptors, even if TIE1 does not dimerize on its own (Figure 4C). Both proposed models would position TIE1 receptors in close spatial proximity, thereby increasing the cytosolic signaling strength of the TIE1 kinase domains upon binding of SVEP1 and ANG1/2. While the models put forth are of good quality, further experimentation is needed to confirm the structural model of SVEP1, TIE1, and ANG1/2 multimerization proposed.

Discussion

TIE1 has long been considered an orphan receptor. Recently, we and others have shown that *svep1* and *tie1* genetically interact (Hußmann et al. 2023) and that SVEP1 binds to murine and human TIE1 (Hußmann et al. 2023; Sato-Nishiuchi et al. 2023). Here, we extend the analysis of SVEP1 as a binding ligand for TIE1 with the assistance of AF3 modeling and experimental support that demonstrates potentiated recruitment of TIE1 by SVEP1 in the presence of angiopoietins.

It is known that TIE2 is activated through binding of angiopoietins, including ANG1 and ANG2 (Davis et al. 1996; Maisonpierre et al. 1997), and that in humans and mice, angiopoietins do not directly bind to TIE1. In zebrafish, however, Ang1 binds to Tie1, Tie2 mutants do not have an obvious cardiovascular phenotype, and the *tie2* locus has been lost in many teleost species (Jiang et al. 2020). Therefore, zebrafish differ from humans and mice in terms of the TIE pathway, as zebrafish appear to exclusively use Tie1 and not Tie2 (Gjini et al. 2011; Jiang et al. 2020; Morooka et al. 2024). Both SPR testing and AF3 modeling revealed that SVEP1 (CCP15-CCP24) does not interact with TIE2. This is in line with trans-well migration assays, which revealed that SVEP1 induces the migration of lymphatic endothelial cells through binding to TIE1, but not TIE2 (Sato-Nishiuchi et al. 2023). Whether TIE2 is able to bind SVEP1 in a condition where other proteins like angiopoietins are present is still a question of interest and requires further investigation.

We here demonstrate via AF3 model and co-immunoprecipitation, that the affinity of TIE1 for SVEP1 is highly enhanced by the simultaneous binding of the C-terminal domains of ANG2 to the CCP20 module, thus generating a complex of SVEP1, angiopoietins, and TIE1 molecules in which the angiopoietins are also able to bind TIE1. Utilizing AF3 modeling, we were able to confidently predict an interaction hub with a 2:2:2 complex of SVEP1, TIE1, and ANG1/2, where ANG1/2 binds different SVEP1 molecules by cross-lacing of N-terminal coiled-coil dimers, which then brings several TIE1 receptors into spatial proximity on the cell surface. This could lead to a cumulative increase in the signal strength of the cytosolic kinase TIE1. While TIE2 has been shown to dimerize via Fn3-Fn3' contacts (Moore et al. 2017), evidence of TIE1 dimerization is limited. Leppanen et al. (2017) captured a strand swapped dimer of TIE1 Fn3 by X-ray crystallography (pdb: 5N06). However, solution SAXS data indicated monomeric TIE1 Fn3, leading to the conclusion that the observed crystallography dimer is likely to be a crystal artifact. However, our model as well as experimental data predicts that in presence of SVEP1 and ANG1, TIE1 can dimerize and thus is phosphorylated upon ligand binding. So far, phosphorylation of TIE1 has not been detected when cells were stimulated with either SVEP1 or ANG2 only (Saharinen et al. 2005; Sato-Nishiuchi et al. 2023; Savant et al. 2015). Sato-Nishiuchi et al. (2023) could not detect an increase in the baseline phosphorylation of murine TIE1 in either LECs or 293-F cells that were treated with Svep1. Only TIE2 co-expression increased TIE1 phosphorylation irrespective of the presence or absence of Svep1. In blood and lymphatic endothelial cells, only COMP-Ang1 and ANG1 have been shown to stimulate the phosphorylation of TIE1 (Saharinen et al. 2005; Savant et al. 2015; Yuan et al. 2007). Co-transfection of TIE1 and TIE2 enhances TIE1 activation and phosphorylation due to heteromeric TIE1-TIE2 complexes. On the contrary, TIE2 phosphorylation is not enhanced by the presence of TIE1 (Saharinen et al. 2005), and TIE1 is not phosphorylated

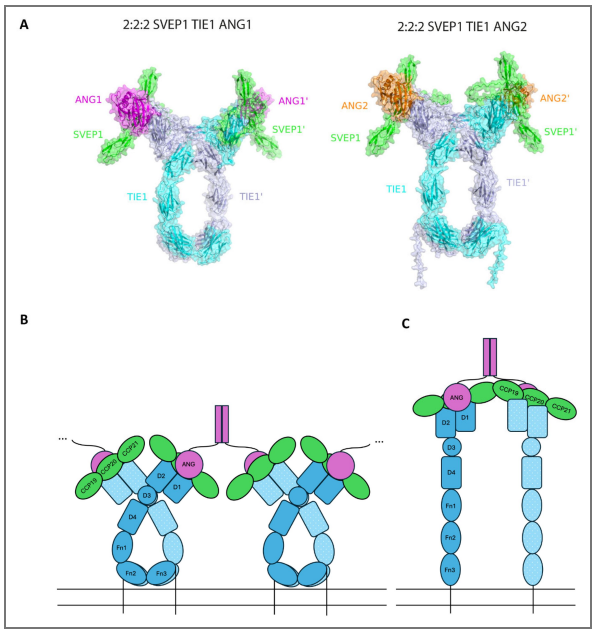

Figure 4. SVEP1, TIE1 and ANG1/2 can form 2:2:2 complexes mediated by SVEP1.

(**A**) Larger hexameric complexes of SVEP1-TIE1 D1-D4-ANG1/2 in a 2:2:2 stoichiometry could be confidently modeled with AF3. They show a symmetric assembly linked by predicted TIE1 dimerization sites at FN3-FN2' as well as the D3 and D4 domains. Similar to the 1:1:1 complex of SVEP1-TIE1-ANG1/2, ANG1/2 makes contact with the D1 and D2 domains of TIE1 by inclusion of the SVEP1 chain (CCP19-21). (**B**) Schematic model of SVEP1 enabling the multimerization of TIE1 receptors on the cell surface by cross-lacing of TIE1 dimers and N-terminal coiled-coil dimers (or greater assemblies) of ANG1/2. (**C**) Schematic model of TIE1 clustering via only ANG1/2 mediated multimerization.

in the absence of TIE2 upon ANG1 stimulation (Savant et al. 2015). According to current knowledge, the phosphorylation of TIE1 is therefore dependent on TIE2. In zebrafish, however, it was shown that Tie1 can be phosphorylated (Morooka et al. 2024) and that Tie1, not Tie2, is the relevant receptor for lymphangiogenesis during early development. Furthermore, it was reported that autophosphorylation of TIE1 (Y1007) is not dependent on TIE2 but on TIE1, because substitutions in the kinase domain of TIE1 result in a loss of its baseline phosphorylation (Brouillard et al. 2024). Additionally, after COMP-Ang1 stimulation of TIE1-transfected 293T cells that do not express TIE2, weak phosphorylation is observed, whereby the activation is mediated by ANG1 and not by the COMP domain, a minimal coiled-coil segment that oligomerizes the ANG1 C-term module (Saharinen et al. 2005), which suggests that the phosphorylation is not dependent on TIE1/TIE2 heterodimerization. Nevertheless, since TIE1 was considered an orphan receptor during that time, the result could not be explained in 2005, and it was speculated whether COMP-Ang1–induced Tie1 activation could involve complex formation with additional molecules.

Our results show phosphorylation of TIE1 after combined SVEP1-ANG2 stimulation of hdLECs. SVEP1 is not expressed by HUVECs and LECs, but in non-endothelial cells (such as fibroblasts) in close proximity to LECs (Karpanen et al. 2017; Hußmann et al. 2023; Wang et al. 2020). According to data from the human protein atlas (*https://www.proteinatlas.org*), SVEP1 is also not expressed in HEK293 cells. Since SVEP1, which is necessary for the phosphorylation of TIE1, is provided by cells in the immediate vicinity of ECs and not by ECs themselves, the phosphorylation of TIE1 after ANG2 stimulation was never detected in cell culture experiments without SVEP1 being present. Whether TIE2 is necessary for the phosphorylation of TIE1 after SVEP1-ANG2 treatment needs further investigation. Our model shows that after binding of SVEP1 to TIE1, ANG1/2 are then able to dock onto this complex, and serve as a 'molecular glue' for both SVEP1 and TIE1. Thus, TIE1-bound SVEP1 would serve as a cell-surface-tethered interaction hub for angiopoietins that are oligomerized – by either the native coiled-coil extensions or the minimal COMP domain – and create cross-linked fields of signaling TIE1 receptors (Figure 4).

The PI3K/Akt signaling pathway is involved in Svep1-induced LEC migration, as LECs show an increased Akt phosphorylation after Svep1 treatment (Sato-Nishiuchi et al. 2023). We were able to show that combined SVEP1-ANG2 stimulation leads to an even higher phosphorylation of AKT in human LECs than the sum of SVEP1 or ANG2 stimulations alone. Blocking of ANG2 using a function blocking antibody prevents AKT phosphorylation after stimulation with SVEP1, implying that SVEP1 cannot induce downstream signaling on its own, but only in combination with angiopoietins.

Furthermore, both TIE1 and TIE2 are required for the full signaling potential of SVEP1-ANG2, as knock-down of either TIE1 or TIE2 reduced the phosphorylation of AKT upon SVEP1-ANG2 stimulation. A signaling event downstream of PI3K/Akt is the inactivation and nuclear exclusion of FOXO1 (Daly et al. 2004), which is reduced in Tie1-silenced vascular endothelial cells (Korhonen et al. 2016). Furthermore, SVEP1 induces FOXO1 nuclear exclusion. This was shown in LECs as well as *in situ* where FOXO1 immunostaining of lymphatic vessels in wild type mice was detected in the nucleus, whereas in *Svep1*-deficient mice, FOXO1 staining was detectable in both the nucleus and cytoplasm (Sato-Nishiuchi et al. 2023). During secondary sprouting of endothelial cells in the zebrafish trunk, Tie1 induces nuclear exclusion of *foxo1a*, since *tie1* mutants displayed an enhanced localization of *foxo1a* in the nucleus (Morooka et al. 2024). Thus, the nuclear versus cytoplasmic ratio of FOXO1 is used as a readout for signaling in a number of systems. Here we show that stimulation of LECs with a combination of SVEP1 and ANG2 leads to a stronger nuclear exclusion of FOXO1 than with either factor alone, thus indicating that stronger binding of SVEP1 to TIE1 also potentiates downstream signaling of TIE1.

The CCP20 module of SVEP1 acts as a critical binding partner for TIE1, but not TIE2, when interacting with ANG1/2. However, it remains unclear whether TIE2 could bind to other sites of SVEP1 in the presence of other proteins, since in the SPR assay and the immunoprecipitation assays, only part of the C-terminus of the SVEP1 protein was used. Also, TIE1 but not TIE2 is required for SVEP1-induced migration (Sato-Nishiuchi et al. 2023), but both are necessary for SVEP1-stimulated phosphorylation of AKT. Furthermore, in capillaries, only depletion of *Tie1*, but

not of *Tie2*, had an effect, whereas in collecting vessels, depletion of *Tie2* resulted in a phenotype (Korhonen et al. 2022). This result can most likely be explained by high expression levels of TIE2 in collecting vessels, but low expression levels of TIE2 in capillaries. Additionally, it is proposed that SVEP1 acts as a modifier of TIE2 expression during Schlemm's canal development as patients that are trans-heterozygous for TIE2 and SVEP1 develop glaucoma and the p.R997C-SVEP1 variant, which is mutated in some glaucoma patients and located shortly after the Furin cleavage site, fails to enhance TIE2 expression in HEK293T cells compared to wild type SVEP1 (Young et al. 2020). Depending on the downstream signaling event as well as the lymphatic cell type (capillaries versus collecting vessels), TIE2 might be needed for phosphorylation of TIE1 either independently of SVEP1 or for binding to other domains of SVEP1 than CCP19-21.

The activation mechanisms of the TIE receptors have long been a point of contention. Especially TIE1 activation and how possible signaling occurs has remained enigmatic, and only recently SVEP1 has been demonstrated to serve as a ligand for the TIE1 transmembrane receptor, which for many years had been considered an orphan receptor with phosphorylation believed to be dependent on TIE2. We here show that SVEP1-ANG2 is able to cause phosphorylation of TIE1 and show that the presence of ANG2 results in stronger recruitment of TIE1 to SVEP1, supporting a model that predicts a higher order complex of SVEP1, TIE1, and ANG1/2. In such complexes, ANG1/2 binds different SVEP1 molecules by cross-lacing of N-terminal coiled-coil dimers, which then brings several TIE1 receptors into spatial proximity on the cell surface. This could lead to formation of a signaling hub, where the signal strength of the cytosolic kinase TIE1, or another signaling moiety, is increased.

Material and Methods

Key Resources Table				
Reagent type (species) or resource	**Designation**	**Source or reference**	**Identifiers**	**Additional information**
cell line (*homo sapiens*)	HEK293 EBNA	Manuel Koch		
cell line (*homo sapiens*)	293T HEK cells	Roukens et al. 2015		
cell line (*homo sapiens*)	Human Dermal Lymphatic Endothelial Cells	PromoCell	C-12216	

transfected construct (*homo sapiens*)	TIE1-HA in PCEP4	Hußmann et al. 2023		TIE1 cDNA provided by Hellmut Augustin
transfected construct (*homo sapiens*)	TIE2-HA in PCEP4	Hußmann et al. 2023		provided by Manuel Koch
transfected construct (*homo sapiens*)	ANG1-FLAG	This paper		provided by Manuel Koch
transfected construct (*homo sapiens*)	ANG2-FLAG	This paper		provided by Manuel Koch
Peptide, recombinant protein	VEGF-C	R&D	9199-VC	
Peptide, recombinant protein	Human recombinant protein ANG1	R&D Systems	923-AN-025	
Peptide, recombinant protein	Human recombinant protein ANG2	R&D Systems	623-AN-025	
Peptide, recombinant protein	Human ANG1 - Strep II (amino acids (aa) 20-497)	This paper		provided by Manuel Koch
Peptide, recombinant protein	Human ANG2 - Strep II (aa 20-495)	This paper		provided by Manuel Koch
Peptide, recombinant protein	Human C-term SVEP1- Strep II purified recombinant protein, reaching from CCP15 to the C-Term, aa 2261-3572	Hußmann et al. 2023		provided by Manuel Koch

Peptide, recombinant protein	Human C-term SVEP1 TIE1mut-Strep II purified recombinant protein, reaching from CCP15 to the C-Term,aa 2261-3572, mutation E2568A G2569A)	This paper		provided by Manuel Koch
Peptide, recombinant protein	Human complete C-term SVEP1 Strep II purified recombinant protein, reaching from EGF1 to the C-Term, aa 919 to the C-term	This paper		provided by Manuel Koch
Peptide, recombinant protein	TIE1 (ectodomain TIE1, aa: 21-760)	This paper		provided by Manuel Koch
Peptide, recombinant protein	TIE2 (ectodomain TIE2, aa: 23-745)	This paper		provided by Manuel Koch
Peptide, recombinant protein	TIE1- Strep II ALFA-tag (ectodomain TIE1, aa: 21-760)	This paper		provided by Manuel Koch
Peptide, recombinant protein	SVEP1-Strep II CCP domain 19_20_21 Purified recombinant protein (aa 2496 – 2714)	This paper		provided by Manuel Koch
Peptide, recombinant protein	SVEP1-Strep II CCP domain 19_20 Purified recombinant protein (aa 2496-2610)	This paper		provided by Manuel Koch
Peptide, recombinant protein	SVEP1-Strep II domain 19_20mut_21	This paper		provided by

	Purified recombinant protein (aa 2496 – 2714, E2568A G2569A))			Manuel Koch
Peptide, recombinant protein	VEGFC-Strep II Purified recombinant protein	This Paper		provided by Manuel Koch
antibody	anti-HA (rat, monoclonal)	Roche	11867423001	1:10000
antibody	anti-FLAG (rabbit, polyclonal)	Sigma-Aldrich	F1804	1:10000
antibody	Strep-Tactin® HRP conjugate	Iba-lifesciences	2-1502-001	1:10000
antibody	anti-goat (donkey, polyclonal) 488	Thermo Scientific	A11055	1:500
antibody	anti-mouse (donkey, polyclonal) 546	Thermo Scientific	A-21123	1:500
antibody	anti-rabbit (donkey, polyclonal) 647	Thermo Scientific	A31573	1:500
antibody	anti-mouse (donkey, polyclonal) HRP	Jackson Immuno Research	715-035-150	1:15000
antibody	anti-goat (donkey, polyclonal) HRP	Immuno Reagents Inc.	DkxGt-003-EHRPX	1:15000
antibody	anti-rabbit (donkey polyclonal) HRP	Jackson Immuno Research	711-035-152	1:15000
antibody	anti-TIE2 (goat, polyclonal)	R&D Systems	AF313	1:300
antibody	anti-TIE1 (goat, polyclonal)	R&D Systems	AF619	1:300

antibody	anti–phospho-TIE2 (rabbit, polyclonal)	R&D Systems	pY992, AF2720	1:300
antibody	anti-phosphotyrosine (mouse, monoclonal)	Millipore	05-321, clone 4G10,	1:500
antibody	Phospho-AKT (S473) (rabbit, polyclonal)	Cell Signaling Technology	9271	
antibody	anti-total AKT (mouse, monoclonal) anti-total AKT (rabbit, polyclonal)	Cell Signaling Technology	2920, 9272	
antibody	phospho-ERK	Cell Signaling Technology	43705	1:2000
antibody	total ERK (mouse, monoclonal)	Cell Signaling Technology	4696	1:4000
antibody	ZO-1 (mouse, monoclonal)	Thermo Scientific	33-9100	1:300
antibody	FOXO1(rabbit, monoclonal)	Cell Signaling	C29H4, 2880	1:300
antibody	HSC70 (mouse, monoclonal)	Sigma-Aldrich	MABE1120	1:1000
antibody	Anti-ANGPT2 (MEDI3617)	Selleckchem	A2770	
chemical compound, drug	Pierce™Avidin	Thermo Scientific	21121	
chemical compound, drug	Endothelial Cell Growth Medium MV2	PromoCell	C-22022	

chemical compound, drug	Endothelial Cell Growth Medium MV2	PromoCell	C-39226	
chemical compound, drug	FCS	Merck Chemicals GmbH	F7524	
chemical compound, drug	DMEM/F-12, GlutaMAX™ Supplement	Thermofisher Scientific	10565018	
chemical compound, drug	fibronectin (1ug/mL)	Sigma	F1141-1MG	
chemical compound, drug	SuperSignal™ West Pico PLUS Chemilumineszenz -Substrat	Thermo Fisher Scientific	34580	
chemical compound, drug	Fluormount-G	Thermo scientific	00-4958-02	
chemical compound, drug	Strep-Tactin® Superflow® high capacity resin	IBA Lifesciences GmbH	2-1208-002	
chemical compound, drug	Lipofectamin 2000 transfection reagent	ThermoFisher Scientific	11668030	
chemical compound, drug	1-phenyl-2-thiourea (75 mM)	Sigma	P7629	
chemical compound, drug	tricaine	Sigma	A5040	
chemical compound, drug	0.8% low melting agarose	Thermo Fischer	16520100	
chemical compound, drug	protein G–Sepharose	GE Healthsciences	GE17-0618-01	
chemical compound, drug	PrimeSTAR® Max DNA Polymerase	TaKaRa	R045A	

Commercial assay, kit	QIAquick PCR purification kit	QIAGEN	28106	
Commercial assay, kit	GeneJET gel extraction kit	ThermoScientific	K0503	
chemical compound, drug	DpnI,	Promega	R623A	
chemical compound, drug	AvrII	New England Biolabs	R0174S	
chemical compound, drug	T4 DNA Ligase (1-3u/µl)	Promega	M180A	
chemical compound, drug	T7 RiboMAX TM Large Scale RNA Production System	Promega	#P1280	
chemical compound, drug	Ribo m7G Cap Analog	Promega	#P1711	
chemical compound, drug	2x rapid ligation buffer	Promega	#C671A	
chemical compound, drug	10x ligation buffer	Promega	#C126B	
cells	Promega JM109 Competent E. coli	Promega	#L1001	
cells	NEB® 5-alpha Competent E. coli	Promega	#C2987	
software, algorithm	R Studio	2023.06.0 Build 421		
software, algorithm	Fiji-ImageJ	(version 1.54 f)		

software, algorithm	ZEISS Elyra 7 superresolution microscope			
software, algorithm	ZEN Microscopy Software	Zen blue and Zen black		
software, algorithm	Leica	LAS X 3.5.7.23225		
software, algorithm	Adobe Illustrator	2023		
software, algorithm	Arivis	Vision 4D 4.1		
software, algorithm	AlphaFold2-multimer (AF2.3.2)	accessed via ColabFold 1.5.5 (https://github.com/sokrypton/ColabFold)		
software, algorithm	DeepMind portal	(https://alphafoldserver.com/).		
software, algorithm	Predictome web site	ahttps://predictomes.org/tools/af3/		
software, algorithm	PyMOL3.04	http://www.pymol.org		
Sequence-based reagent	TIE1 siRNA	IDT	234070784	hs.Ri.TIE1.13
Sequence-based reagent	TEK siRNA	Thermo Fisher Scientific	Catalog #4390824, Catalog #4392420,	siRNA ID #s13984, siRNA ID #s224717
Other	Immobilon-P Membrane, PVDF	Millipore Thermo	IPVH00010	

Recombinant protein expression

Recombinant proteins (SVEP1, GenBank: NM_153366.5), (ANG1, GenBank: NM_001199859), (ANG2, GenBank: NM_001118887), TIE1 (GenBank: NM_005424) and TIE2 (GenBank: NM_000459) were amplified from human cDNA by PCR. Amino acids contained in the different recombinant proteins are listed in the key resource table. Protein production was carried out essentially as described (Hußmann et al. 2023; Meier et al. 2023). Briefly, SVEP1, TIE1 and ANG2 containing an N-terminal twin Strep-tag were expressed in HEK 293 T cells using the inducible sleeping beauty

transposon system and secreted into the medium. Tagged proteins were bound to Strep-Tactin XT 4Flow matrix (IBA Lifescience) equilibrated in 50 mM Tris pH 8.0, 150 mM NaCl. After washing with 50 mM Tris pH 8.0, 1 M NaCl proteins were recovered using Biotin containing BXT elution buffer (IBA Lifescience) and subsequently dialyzed into PBS. PCR products were cloned into a modified sleeping beauty transposon expression vector containing a BM40 signal peptide sequence and a Twin-Strep-tag. For recombinant protein production, stable HEK293 EBNA cell lines were generated employing the sleeping beauty transposon system (Kowarz et al. 2015). Briefly, expression constructs were co-transfected with a transposase plasmid (1:10) into the HEK293 EBNA cells using FuGENE HD transfection reagent (Promega). After selection with puromycin (2 µg/ml), cells were induced with doxycycline. Supernatants were filtered and the recombinant proteins purified via Strep-Tactin®XT (IBA Lifescience) resin. Proteins were then eluted by biotin-containing TBS-buffer (IBA Lifescience) and subsequently dialyzed into PBS. The human sequences of *ANGPT1* (corresponding to NM_001199859, aa: 20 – 497) and *ANGPT2* (corresponding to NM_001118887, aa: 20–495) were cloned into the PCEP episomal expression system (transient) including an N-terminal Flag-tag sequence.

Surface Plasmon Resonance

Protein-protein interactions were analyzed by surface plasmon resonance (SPR) experiments using a Biacore T200 system (Cytiva, Uppsala, Sweden). Human active SVEP1-Strep II recombinant protein, reaching from CCP15 to the CCP24, aa 2261-2890 and TIE1 (ectodomain TIE1, aa: 21-760) or TIE2 (ectodomain TIE2, (aa: 23-745) were used. For immobilization of hSVEP1, a CM5 sensor chip was activated with N-hydroxysuccinimide (NHS) and 1-ethyl-3-(3-dimethylaminopropyl) carbodiimide hydrochloride (EDC) according to the manufacturer's instructions, and 2050 response units (RU) of SVEP1 were coupled in 10 mM sodium acetate buffer, pH 4.0, at a flow rate of 10 µL/min. For the interaction measurements, the analytes, TIE1 and TIE2, were passed over the sensor chip at a flow rate of 30 µl/min in running buffer (10 mM HEPES, 150 mM NaCl and 0.005% Tween20). The concentrations for the TIE proteins were 200 nM, 100 nM, 50 nM, 25 nM, 12.5 nM, 6.25 nM and 3.125 nM. The binding kinetics were calculated by fitting a 1:1 interaction model using the BIAevalution software (Cytiva, Uppsala, Sweden).

Negative staining

The interaction of the SVEP1 C-terminus with Angiopoietin 1 was visualized by negative staining and transmission electron microscopy. Briefly, the proteins were incubated for 1 hour at 37°C in Tris-buffered saline (TBS), pH 7.4. Prior to the visualization in the electron microscope, the proteins were negatively stained with 1% uranyl acetate on the grids. In some experiments, the proteins were directly labelled with 5 nm (Sigma-Aldrich 752568) and 10 nm (Sigma-Aldrich 752584) colloidal gold, respectively, as previously described (Baschong and Wrigley 1990). Specimens were examined in a Philips/FEI CM 100 TWIN transmission electron microscope operated at 60 kV accelerating voltage. Images were recorded with a side-mounted Olympus Veleta camera with a resolution of 2048 × 2048 pixels (2k × 2K) and the ITEM acquisitions software.

ELISA binding assays

ELISA assays were performed as described (Eble 2018; Meier et al. 2023). Briefly, SVEP1 or SVEP1 mutants (2 µg/ml in TBS) were coated on 96 well plates (Nunc MaxiSorp, 50 µl/well) for 1 h at room temperature and subsequently washed with TBS. Plates were blocked using Pierce Protein-Free Blocking Buffer (ThermoFisher Scientific) for 1 h at room temperature followed by 1 % BSA in TBS over night at 4°C. Bound SVEP1 was overlaid with serial dilutions of TIE1 in the presence or absence of ANG2, or TIE mutant containing an ALFA tag, or biotinylated ANG2 protein, and incubated for 1 h at room temperature. After washing with PBS, protein complexes were fixed with 2.5 % glutaraldehyde in PBS for 10 min and the reaction stopped by washing with TBS. Bound TIE or ANG2 proteins were detected with HRP conjugated anti ALFA-tag nanobody or anti-Biotin antibody and stained using 1-Step Ultra TMB-ELISA (ThermoFisher Scientific). After addition of

10% sulfuric acid, absorbance reading at 450 nm was done on a Tecan plate reader equipped with Magellan Pro software. Non-linear regression analysis of data was performed using GraphPad Prism 11 software.

Cell culture and treatment/stimulation

HEK293T cells were cultured in DMEM (Thermo Fisher Scientific #61965026) and seeded one day before transfection utilizing Lipofectamine™ 2000 (Thermo Fisher Scientific, #11668027). hdLECs (Human Dermal Lymphatic Endothelial Cells, PromoCell) were cultured in Endothelial Cell Growth Medium MV2 (PromoCell, #C-22022) on Fibronectin-coated (Sigma, #F1141-1MG, 1ug/mL) culture flasks. LEC culture medium was supplemented with 25 ng/ml VEGF-C (R&D, #9199-VC). Cells were seeded on ibidi slides (ibidi, #81201) and grown to confluency before the treatment.

For knock-down experiments, hdLECs were transfected with *TIE1*, *TIE2* or control siRNA (see key resources table) using Lipofectamine™ RNAiMAX Transfection Reagent one day after splitting and two days prior to analysis of AKT phosphorylation.

For the pull-down assay, different versions of human StrepII tagged SVEP1 protein and a StrepII tagged control protein were incubated with 25 µl Strep-TactinXT 4Flow high-capacity resin (iba-lifesciences, #2-5030-002) in 500 µl binding buffer (50 mM Tris–HCl at pH 7.5, 100 mM NaCl, 0.02% Triton X-100) for 30 min. Subsequently, the cell lysate of TIE1-HA transfected HEK293T cells was added. After 2 hours of incubation, the beads were washed 5 times with Ripa buffer (50 mM Tris (pH 7.5), 1% NP-40, 0,1% SDS, 0,5% Na-deoxycholate, 150 mM NaCl) and boiled for 5 min at 95°C in sample buffer. For pull down assays that include angiopoietins, TIE1-HA and ANG2-FLAG/ANG1-FLAG were co-transfected and the cell lysates were pre-cleared with Strep-TactinXT 4Flow high-capacity resin, before adding them to the StrepII tagged SVEP1 protein.

For TIE1 autophosphorylation, hdLECs were starved for 3 hours in 0.5% BSA-containing MV2 medium, followed by 1 hour of stimulation with ANG2 and SVEP1 alone or in combination. The cells were lysed in PLCLB lysis buffer (150 mM NaCl, 5% glycerol, 1% Triton X-100, 1.5 mM MgCl2, 2mM CaCl2, 50 mM HEPES, pH 7.5, 1 x Complete-EDTA-free proteinase inhibitors) followed by TIE1 immunoprecipitation using anti-TIE1 antibodies (AF619, R&D Systems) and protein G–Sepharose (GE Healthsciences Ab, #GE17-0618-01) at +4°C. After 2 hours of incubation, the beads were washed 5 times with PLCLB lysis buffer and boiled for 5 min at 95°C in sample buffer.

For analysis of pAKT, growth medium of confluent hdLECs was changed to MV2 medium containing growth supplements but lacking VEGFC. Cells were starved for 3 hours in 0.5% BSA-containing MV2 medium, followed by 40-60 minutes of stimulation with ANG2 (0.5 µg/mL) and/or SVEP1 (1 µg/mL). Cells were treated with anti-ANG2 antibody (2 µg/ml; MEDI3617 A2770, Selleckchem) for 2 h prior to stimulation with SVEP1. The cells were lysed in lysis buffer (20 mM Tris-HCl (pH 7.4), 150 mM NaCl, 2mM CaCl2, 1.5 mM MgCl2, 1 mM Na3VO4, 1 % (v/v) Triton-X-100, 0.04 % (w/v) NaN3, 1 x Complete-EDTA-free proteinase inhibitors) or PLCLB lysis buffer and centrifuged before gel analysis.

Western blot

Cell lysates and cell precipitates were subjected to Western blot analysis by separation in SDS-page and blotting onto PVDF membrane. Blots were probed with primary antibodies followed by HRP coupled secondary antibodies and ECL detection (SuperSignal™ West Pico PLUS Chemilumineszenz-Substrat, Thermo Fisher Scientific, 34580). Blots were imaged using an Odyssey FC (LICOR). Primary and secondary antibodies used for analysis are listed in the key resources table and are stated in the figure of the respective blot. Before using the Strep-Tactin® HRP antibody, the membrane was incubated in 2,5µg/ml Avidin (biotin blocking solution) for 10 minutes. HSC70 was used to assure equal loading of the gels and values were normalized by the level of HSC70.

Immunocytochemistry and imaging

Before the treatment, hdLECs were starved for 4 hours in MV2 medium without supplements and with 0,5 % FBS. After treatment with SVEP1 and/or ANG2 (623-AN R&D Systems) for 1-hour cells were fixed with 4 % PFA for 10 minutes. Afterwards the fixed cells were permeabilized using 0,5% TritonX-100 in PBS for 5 minutes and blocked with 2% BSA for 1 hour. Incubation of the slides with the antibody was conducted over night at 4°C (ZO-1 (Thermo Scientific, 33-9100), FOXO1 (Cell Signaling, C29H4, #2880)). After washing the slides several times with 0,1%PBS-TritonX100 the secondary antibody staining was conducted at room temperature for 50 minutes (Donkey-anti-rabbit-647 (Thermo Scientific A31573), Donkey-anti-mouse-546 (Thermo Scientific), DAPI). Slides were washed and mounted using Fluormount-G (Thermo scientific 00-4958-02). Images were taken using ZEISS Elyra 7 super-resolution microscope in Apotome mode with 20x objective and processed with ZEN Microscopy Software (Zen blue 3.5 and Zen black). ZEISS arivis Software was used to calculate the pixel intensities inside the nucleus and in the cytoplasm. ZO1 was used to identify single cells and the ratio was calculated for each cell.

Statistics and reproducibility

Data sets were tested for normality (Shapiro–Wilk) and equal variance. P-values of data sets with normal distribution were determined by Student's *t*-test. In case data values did not show normal distribution, a Mann–Whitney U test was performed instead. For multiple comparison the p values were adjusted with Bonferroni correction. Results are presented as mean ± SD. Statistical tests were performed using GraphPad Prism 8 and R. For visualizations, the R package ggplot2 was used. All experiments were carried out at least three times. P values > 0.05 were considered not significant. * p≤0.05, ** p≤0.01, ***p≤0.001, **** p≤0.0001.

Structure prediction and modeling of SVEP1 complexes

Amino acid sequences for human SVEP1 (*https://www.uniprot.org/uniprotkb/Q4LDE5*), TIE1/2 (*https://www.uniprot.org/uniprotkb/P35590* and /Q02763) and ANG1/2 (*https://www.uniprot.org/uniprotkb/Q15389* and /O15123) were retrieved from UniProtKB. The most recent version of AlphaFold2-multimer (v2.3.2) was accessed via ColabFold (v1.6.1) (*https://github.com/sokrypton/ColabFold*) while the DeepMind portal was used for AF3 (*https://alphafoldserver.com/*) modelling of >2500 amino acid jobs. For the template-free AF2.3 predictions, num recycles=auto and num models=5 were used, models were relaxed with AMBER, and ranked based on ipTM scores; in turn, default parameters were used for AF3. Top ranked model interfaces were analyzed and visualized with PDBePISA (Krissinel and Henrick 2007) and PyMOL v3.1.8 (The PyMOL Molecular Graphics System, Version 3.1.4.1, Schrödinger, LLC).

Supplementary figures

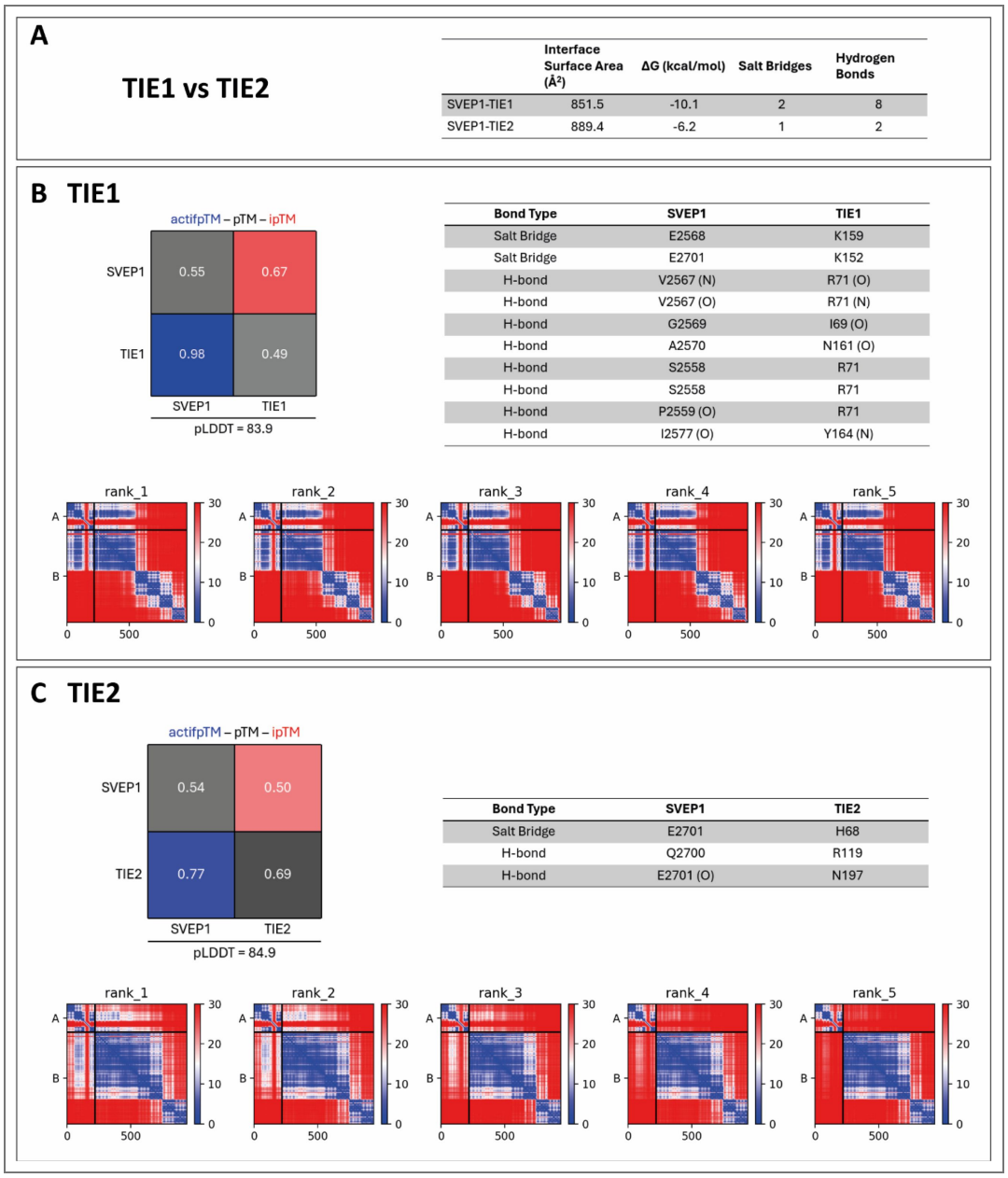

	Interface Surface Area (Å²)	ΔG (kcal/mol)	Salt Bridges	Hydrogen Bonds
SVEP1-TIE1	851.5	-10.1	2	8
SVEP1-TIE2	889.4	-6.2	1	2

Bond Type	SVEP1	TIE1
Salt Bridge	E2568	K159
Salt Bridge	E2701	K152
H-bond	V2567 (N)	R71 (O)
H-bond	V2567 (O)	R71 (N)
H-bond	G2569	I69 (O)
H-bond	A2570	N161 (O)
H-bond	S2558	R71
H-bond	S2558	R71
H-bond	P2559 (O)	R71
H-bond	I2577 (O)	Y164 (N)

Bond Type	SVEP1	TIE2
Salt Bridge	E2701	H68
H-bond	Q2700	R119
H-bond	E2701 (O)	N197

Supplementary figure 1.1. Statistics and (**A**) PDBePISA analysis of a SVEP1-TIE1ectodomain model vs a SVEP1-TIE2 ectodomain model depicting interface surface area, Gibbs free energy, salt bridges and hydrogen bond contacts. (**B**) and (**C**) statistics table, bonds and PAE plot of TIE1 (**B**) or TIE2 (**C**). PAE plot: A =SVEP1 CCP19-21, B=TIE1 or TIE2.

Supplementary Figure 1.2. **SVEP1 TIE1 interfaces.**

(**A**) Salt bridges E2568-K159 and E2701-K152 between SVEP1 CCP20 (green) and D1/D2 of TIE1 ectodomain (cyan). Electrostatic bonds are highlighted in yellow.. (**B**) Hydrogen bond network of SVEP1 CCP20 (green) and D1/D2 of TIE1 ectodomain (cyan). H-bonds are highlighted in white. (**C**) F2566 of SVEP1 (green) fits in the hydrophobic pocket of TIE1 (cyan) partially formed by P202 and L203. (**D** and **E**) Surface electrostatic potential representation of SVEP1 (green) bound to TIE1 (cyan) detailing that the mainly acidic interaction surface of SVEP1 (**D**) is opposed by a basic interaction surface of TIE1 (**E**). (**F** and **G**) Hydrophobicity surface representations of SVEP1 (green) bound to TIE1 (cyan). The hydrophobic side chains of F2566 and F2583 fit into a hydrophobic cavity of TIE1.

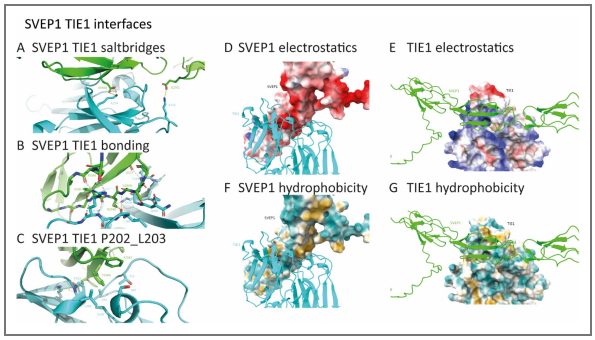

Supplementary figure 1.3.

(**A**) Different versions of human SVEP1-StrepTac (spanning from CCP15 to the C-Term) were immunoprecipitated and associated TIE1 was detected via Western blot analysis. TIE1 bound to CCP19-21 as well as CCP20-21, but not the CCP19-21 mutant containing the E2568A-G2569A mutant or CCP19-20. (**B**) Binding of SVEP1 (wt or E2568A-G2569A) to TIE1 (wt or P202L L203F) was analyzed by ELISA. Both mutations, either in TIE1 or in SVEP1 inhibit binding between TIE1 and SVEP1.

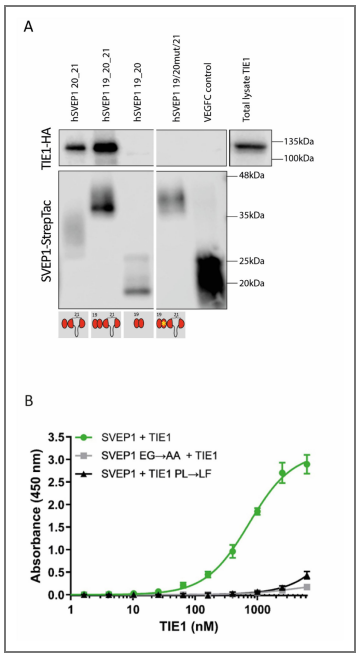

Supplementary figure 2.1.

(**A**) AlphaFold 2.3 multimer output scores and (**B**) PAE plots of SVEP1-TIE1-ANG1/2 complexes. A is SVEP1 CCP19-21, B is TIE1 ecotdomain, C is the ANG1/2 fibrinogen like domain. (**C**) Bonding residues of each interface (**D**) and (**E**) PDBePISA analysis of interfaces of SVEP1-TIE1-ANG1/2 top ranked models. The conformation of the TIE1-ANG1/2 heteromers in the SVEP1-bound pose resembles the solved structures of TIE2 bound to either ANG1 or ANG2. However, the weaker binding of TIE2 to CCP19-21 of SVEP1 fails to nucleate the formation of the TIE2 ternary complex with SVEP1.

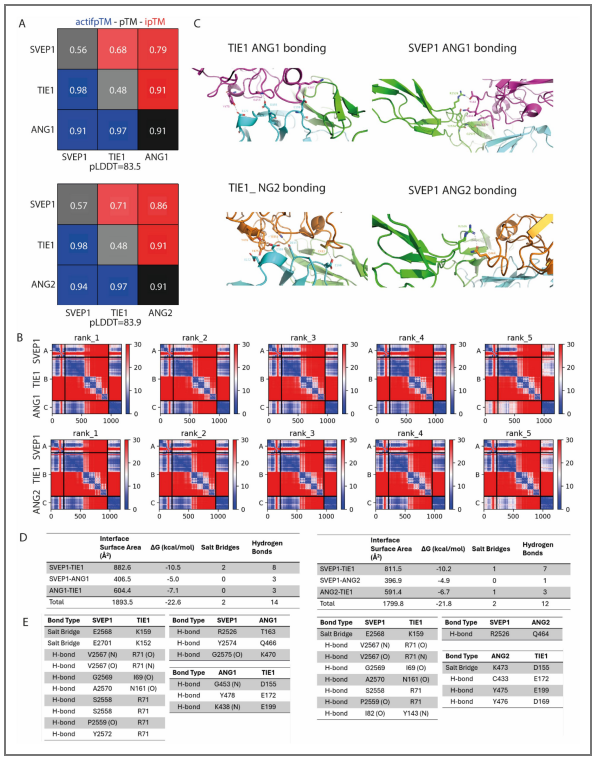

Supplementary figure 2.2.

(A,B,C) Surface electrostatic potential of the interaction surfaces present in the SVEP1-TIE1-ANG1 complex demonstrating complementary charge distributions. (D,E,F) Surface hydrophobicity of the interaction surfaces present in the SVEP1-TIE1-ANG1 complex. (G,H,I) Surface electrostatic potential of the interaction surfaces present in the SVEP1-TIE1-ANG2 complex. (J,K,L) Surface hydrophobicity of the interaction surfaces present in the SVEP1-TIE1-ANG2 complex. All electrostatic potentials and hydrophobicity surfaces were generated and visualized with UCSF Chimera 1.19.

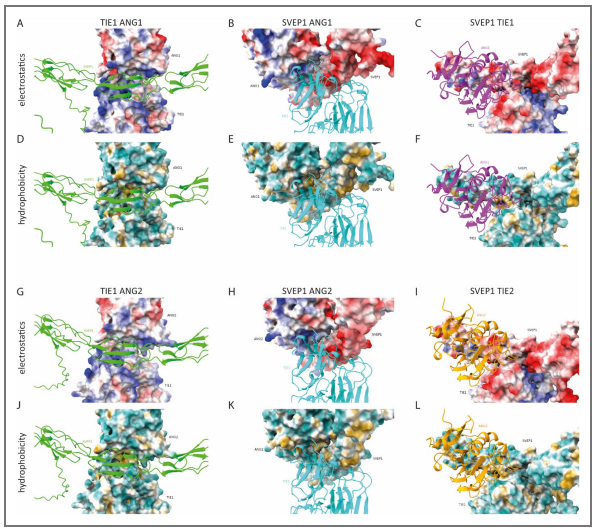

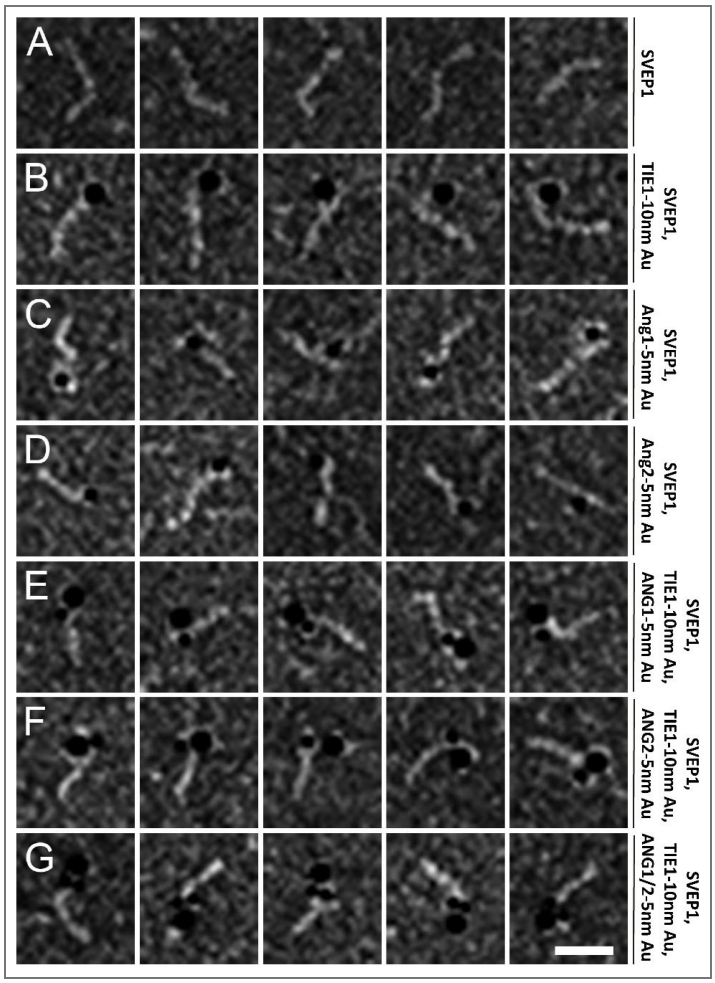

Supplementary figure 2.3. ANG1 and ANG2 bind in close proximity to the site where TIE1 and SVEP1 interact.

Negative staining of human SVEP1 binding to TIE1 with and without the presence of ANG1 or ANG2. (**A**) hSVEP 150 kDa. (**B**) hSVEP-hTIE-10 nm Au. (**C**) hSVEP-ANG1-5nm Au, (**D**) hSVEP-ANG2-5nm Au. (**E**) hSVEP-hTIE-10 nm Au-ANG1-5 nm Au. (**F**) hSVEP-hTIE-10 nm Au-ANG2-5 nm Au. (**G**) hSVEP-hTIE-10 nm Au-ANG1/2-5 nm Au. Parts of panels A and B (control, SVEP1-TIE1-10 nm Au) have also been shown in main figure 1. Scale bar: 25 nm.

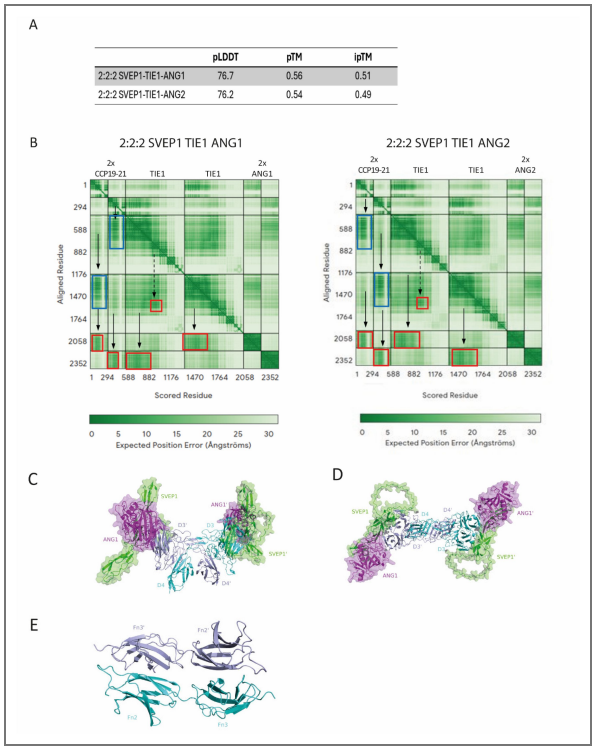

Supplementary Figure 4.1.

(A) AF3 output metrics (B) PAE plots demonstrating confident predictions of the complexes shown in Figure 4. (**C**) and (**D**) The side (**C**) and top (**D**) view of the model hexamer shows the side-by-side, antiparallel packing of TIE1 D3 domains that produces the domain-swapping of D4 Ig domains. **E**) Top view of the Fn2 – Fn3 domains.

Data availability

Scripts used for data analysis available at GitHub at *https://github.com/MuensterImagingNetwork/Uphoff_et_al_2025/tree/main* (copy archived at Münster Imaging Network, 2025). The datasets (eg of images) generated during and/or analyzed during the current study are available from the corresponding author on reasonable request as stated in the manuscript file.

Acknowledgements

This work was supported by the CiM-IMPRS graduate school. We thank Sarah Weischer, Thomas Zobel and Jens Wendt (Münster Imaging Network, Cells in Motion Interfaculty Centre, University of Münster, Germany) for the support in imaging analysis. The Zeiss Elyra 7 microscope was funded by INST 211/901-1 FUGB.

Additional information

Funding

Deutsche Forschungsgemeinschaft (DFG); S.S-M: CRC 1348 project B08, CRC 1607 project C02; M.K. CRC 1607 project Z01 and KO2247/8-2. J.S. Is a Tier-1 Canada Research Chair in Structural Biology and supported by the CRC program. This research was funded by the Canadian Institute of Health Research with the Project Grant CIHR-PJT-178097. The funders had no role in study design, data collection, and interpretation, or the decision to submit the work for publication.

Funding

Funder	Grant reference number	Author
Deutsche Forschungsgemeinschaft (DFG)	CRC 1348 project B08	Stefan Schulte-Merker
Deutsche Forschungsgemeinschaft (DFG)	CRC 1607 project C02	Stefan Schulte-Merker
Deutsche Forschungsgemeinschaft (DFG)	CRC 1607 project Z01	Stefan Schulte-Merker
Deutsche Forschungsgemeinschaft (DFG)	KO2247/8-2	Manuel Koch

Author ORCID iDs

Stefan Schulte-Merker: https://orcid.org/0000-0003-3617-8807

Note

This reviewed preprint has been updated to correct a corresponding email address.

References

Aleström Peter, D'Angelo Livia, Midtlyng Paul J, Schorderet Daniel F, Schulte-Merker Stefan, Sohm Frederic, Warner Susan (2020) Zebrafish: Housing and Husbandry Recommendations. *Laboratory Animals* **54**:213-24 https://doi.org/10.1177/0023677219869037 | PubMed

Baschong W, Wrigley NG (1990) Small colloidal gold conjugated to Fab fragments or to immunoglobulin G as high-resolution labels for electron microscopy: A technical overview. *Journal of electron microscopy technique* **14**:313-323 https://doi.org/10.1002/jemt.1060140405 | PubMed

Bos Frank L, Caunt Maresa, Peterson-Maduro Josi, Planas-Paz Lara, Kowalski Joe, Karpanen Terhi, Van Impel Andreas, et al. (2011) CCBE1 Is Essential for Mammalian Lymphatic Vascular Development and Enhances the Lymphangiogenic Effect of Vascular Endothelial Growth Factor-c in Vivo. *Circulation*

Research **109**:486-91 https://doi.org/10.1161/CIRCRESAHA.111.250738 | PubMed

Brouillard Pascal, Murtomäki Aino, Leppänen Veli Matti, Hyytiäinen Marko, Mestre Sandrine, Potier Lucas, Boon Laurence M, et al. (2024) Loss-of-Function Mutations of the TIE1 Receptor Tyrosine Kinase Cause Late-Onset Primary Lymphedema. *The Journal of Clinical Investigation* **134** https://doi.org/10.1172/JCI173586 | PubMed

Daly Christopher, Wong Vivian, Burova Elena, Wei Yi, Zabski Stephanie, Griffiths Jennifer, Lai Ka Man, et al. (2004) Angiopoietin-1 Modulates Endothelial Cell Function and Gene Expression via the Transcription Factor FKHR (FOXO1). *Genes & Development* **18**:1060-71 https://doi.org/10.1101/GAD.1189704 | PubMed

Davis Samuel, Aldrich Thomas H, Jones Pamela F, Acheson Ann, Compton Debra L, Jain Vivek, Ryan Terence E, et al. (1996) Isolation of Angiopoietin-1, a Ligand for the TIE2 Receptor, by Secretion-Trap Expression Cloning. *Cell* **87**:1161-69 https://doi.org/10.1016/S0092-8674(00)81812-7 | PubMed

Dumont Daniel J, Gradwohl Gérard J, Fong Guo Hua, Auerbach Robert, Breitman Martin L (1993) The Endothelial-Specific Receptor Tyrosine Kinase, Tek, Is a Member of a New Subfamily of Receptors. *Oncogene* **8**:1293-1301 https://europepmc.org/article/med/8386827 | PubMed

Eble Johannes A (2018) Titration ELISA as a Method to Determine the Dissociation Constant of Receptor Ligand Interaction. *J Vis Exp* https://doi.org/10.3791/57334 | PubMed

Gjini Evisa, Hekking Liesbeth H, Küchler Axel, Saharinen Pipsa, Wienholds Erno, Post Jan-Andries, Alitalo Kari, Schulte-Merker Stefan (2011) Zebrafish Tie-2 shares a redundant role with Tie-1 in heart development and regulates vessel integrity. *Disease models & mechanisms* **4**:57-66 https://doi.org/10.1242/dmm.005033 | PubMed

Guen Ludovic Le, Karpanen Terhi, Schulte Dörte, Harris Nicole C, Koltowska Katarzyna, Roukens Guy, Bower Neil I, et al. (2014) Ccbe1 Regulates Vegfc-Mediated Induction of Vegfr3 Signaling during Embryonic Lymphangiogenesis. *Development* **141**:1239-49 https://doi.org/10.1242/DEV.100495

Hansen Tania M, Singh Harprit, Tahir Tariq A, Brindle Nicholas PJ (2010) Effects of Angiopoietins-1 and -2 on the Receptor Tyrosine Kinase Tie2 Are Differentially Regulated at the Endothelial Cell Surface. *Cellular Signalling* **22**:527-32 https://doi.org/10.1016/J.CELLSIG.2009.11.007 | PubMed

Hogan Benjamin M, Herpers Robert, Witte Merlijn, Heloterä Hanna, Alitalo Kari, Duckers Henricus J, Schulte-Merker Stefan (2009) Vegfc/Flt4 Signalling Is Suppressed by Dll4 in Developing Zebrafish Intersegmental Arteries. *Development* **136**:4001-9 https://doi.org/10.1242/dev.039990 | PubMed

Hußmann Melina, Schulte Dörte, Weischer Sarah, Carlantoni Claudia, Nakajima Hiroyuki, Mochizuki Naoki, Stainier Didier YR, Zobel Thomas, Koch Manuel, Schulte-Merker Stefan (2023) Svep1 Is a Binding Ligand of Tie1 and Affects Specific Aspects of Facial Lymphatic Development in a Vegfc-Independent Manner. *eLife* **12**:e82969 https://doi.org/10.7554/ELIFE.82969 | PubMed

Impel Andreas van, Zhao Zhonghua, Hermkens Dorien MA, Guy Roukens M, Fischer Johanna C, Peterson-Maduro Josi, Duckers Henricus, Ober Elke A, Ingham Philip W, Schulte-Merker Stefan (2014) Divergence of Zebrafish and Mouse Lymphatic Cell Fate Specification Pathways. *Development* **141**:1228-38 https://doi.org/10.1242/dev.105031

Jeltsch Michael, Jha Sawan Kumar, Tvorogov Denis, Anisimov Andrey, Leppänen Veli Matti, Holopainen Tanja, Kivelä Riikka, Ortega Sagrario, Kärpanen Terhi, Alitalo Kari (2014) CCBE1 Enhances Lymphangiogenesis via a Disintegrin and Metalloprotease with Thrombospondin Motifs-3-Mediated Vascular Endothelial Growth Factor-C Activation. *Circulation* **129**:1962-71 https://doi.org/10.1161/CIRCULATIONAHA.113.002779 | PubMed

Jiang Zhen, Carlantoni Claudia, Allanki Srinivas, Ebersberger Ingo, Stainier Didier YR (2020) Tek (Tie2) Is Not Required for Cardiovascular Development in Zebrafish. *Development* **147** https://doi.org/10.1242/DEV.193029 | PubMed

Karpanen Terhi, Padberg Yvonne, Van De Pavert Serge A, Dierkes Cathrin, Morooka Nanami, Peterson-Maduro Josi, Van De Hoek Glenn, et al. (2017) An Evolutionarily Conserved Role for Polydom/Svep1 during Lymphatic Vessel Formation. *Circulation Research* **120** https://doi.org/10.1161/CIRCRESAHA.116.308813 | PubMed

Kim Hak-Zoo, Jung Keehoon, Kim Ho Min, Cheng Yifan, Koh Gou Young (2009) A designed angiopoietin-2 variant, pentameric COMP-Ang2, strongly activates Tie2 receptor and stimulates angiogenesis. *Biochimica et Biophysica Acta (BBA)-Molecular Cell Research* **1793**:772-780 https://doi.org/10.1016/j.bbamcr.2009.01.018 | PubMed

Kim Injune, Kim Hwan Gyu, So June-No, Kim Joo Heon, Kwak Hee Jin, Koh Gou Young (2000) Angiopoietin-1 regulates endothelial cell survival through the phosphatidylinositol 3′-kinase/Akt signal transduction pathway. *Circulation research* **86**:24-29 https://doi.org/10.1161/01.res.86.1.24 | PubMed

Kim Kyung-Tae, Choi Han-Ho, Steinmetz Michel O, Maco Bohumil, Kammerer Richard A, Ahn So Young, Kim Hak-Zoo, Lee Gyun Min, Koh Gou Young (2005) Oligomerization and multimerization are critical for angiopoietin-1 to bind and phosphorylate Tie2. *Journal of Biological Chemistry* **280**:20126-20131 https://doi.org/10.1074/jbc.M500292200 | PubMed

Korhonen Emilia A, Lampinen Anita, Giri Hemant, Anisimov Andrey, Kim Minah, Allen Breanna, Fang Shentong, et al. (2016) Tie1 Controls Angiopoietin Function in Vascular Remodeling and Inflammation. *The Journal of Clinical Investigation* **126**:3495 https://doi.org/10.1172/JCI84923 | PubMed

Korhonen Emilia A, Murtomaki Aino, Jha Sawan Kumar, Anisimov Andrey, Pink Anne, Zhang Yan, Stritt Simon, et al. (2022) Lymphangiogenesis Requires Ang2/Tie/PI3K Signaling for VEGFR3 Cell-Surface Expression. *The Journal of Clinical Investigation* **132** https://doi.org/10.1172/JCI155478 | PubMed

Krissinel Evgeny, Henrick Kim (2007) Inference of macromolecular assemblies from crystalline state. *J Mol Biol* **372**:774-97 https://doi.org/10.1016/j.jmb.2007.05.022 | PubMed

Kumar Sanjay Sunil, Uphoff Katharina, Hötte Sophie, Prokosch Verena, Schulte-Merker Stefan, Schulte-Ostermann Dörte (2026) A cellular and molecular perspective on organotypic lymphatic (dys) function. *Seminars in Cell & Developmental Biology* https://doi.org/10.1016/j.semcdb.2025.103665 | PubMed

Leppänen Veli Matti, Saharinen Pipsa, Alitalo Kari (2017) Structural Basis of Tie2 Activation and Tie2/Tie1 Heterodimerization. *Proceedings of the National Academy of Sciences of the United States of America* **114**:4376-81 https://doi.org/10.1073/PNAS.1616166114 | PubMed

Macdonald Philip R, Progias Pavlos, Ciani Barbara, Patel Sanjai, Mayer Ulrike, Steinmetz Michel O, Kammerer Richard A (2006) Structure of the Extracellular Domain of Tie Receptor Tyrosine Kinases and Localization of the Angiopoietin-Binding Epitope. *Journal of Biological Chemistry* **281**:28408-14 https://doi.org/10.1074/JBC.M605219200 | PubMed

Maisonpierre Peter C, Suri Chitra, Jones Pamela F, Bartunkova Sona, Wiegand Stanley J, Radziejewski Czeslaw, Compton Debra, et al. (1997) Angiopoietin-2, a Natural Antagonist for Tie2 That Disrupts in Vivo Angiogenesis. *Science* **277**:55-60 https://doi.org/10.1126/SCIENCE.277.5322.55 | PubMed

Mäkinen Taija, Boon Laurence M, Vikkula Miikka, Alitalo Kari (2021) Lymphatic Malformations: Genetics, Mechanisms and Therapeutic Strategies. *Circulation Research* **129**:136-54 https://doi.org/10.1161/CIRCRESAHA.121.318142 | PubMed

Marron Marie B, Hughes David P, Edge Michael D, Forder Cheryl L, Brindle Nicholas PJ (2000) Evidence for Heterotypic Interaction between the Receptor Tyrosine Kinases Tie-1 and Tie-2. *Journal of Biological Chemistry* **275**:39741-46 https://doi.org/10.1074/jbc.M007189200 | PubMed

Meier Markus, Gupta Monika, Akgül Serife, McDougall Matthew, Imhof Thomas, Nikodemus Denise, Reuten Raphael, Moya-Torres Aniel, To Vu, Ferens Fraser, *et al.* (2023) The dynamic nature of netrin-1 and the structural basis for glycosaminoglycan fragment-induced filament formation. *Nat Commun* **14**:1226 https://doi.org/10.1038/s41467-023-36692-w | PubMed

Moore Jason O, Lemmon Mark A, Ferguson Kathryn M (2017) Dimerization of Tie2 mediated by its membrane-proximal FNIII domains. *Proceedings of the National Academy of Sciences* **114**:4382-4387 https://doi.org/10.1073/pnas.1617800114 | PubMed

Morooka Nanami, Futaki Sugiko, Sato-Nishiuchi Ryoko, Nishino Masafumi, Totani Yuta, Shimono Chisei, Nakano Itsuko, Nakajima Hiroyuki, Mochizuki Naoki, Sekiguchi Kiyotoshi (2017) Polydom Is an Extracellular Matrix Protein Involved in Lymphatic Vessel Remodeling. *Circulation Research* **120**:1276-88 https://doi.org/10.1161/CIRCRESAHA.116.308825 | PubMed

Morooka Nanami, Gui Ning, Ando Koji, Sako Keisuke, Fukumoto Moe, Hasegawa Urara, Hußmann Melina, Schulte-Merker Stefan, Mochizuki Naoki, Nakajima Hiroyuki (2024) Angpt1 Binding to Tie1 Regulates the Signaling Required for Lymphatic Vessel Development in Zebrafish. *Development* **151** https://doi.org/10.1242/DEV.202269 | PubMed

Partanen Juha, Armstrong Elina, Mäkelä Tomi P, Korhonen Jaana, Sandberg Minna, Renkonen Risto, Knuutila Sakari, Huebner Kay, Alitalo Kari (1992) A Novel Endothelial Cell Surface Receptor Tyrosine Kinase with Extracellular Epidermal Growth Factor Homology Domains. *Molecular and Cellular Biology* **12**:1698-1707 https://doi.org/10.1128/MCB.12.4.1698-1707.1992 | PubMed

Petrova Tatiana V, Koh Gou Young (2018) Organ-Specific Lymphatic Vasculature: From Development to Pathophysiology. *Journal of Experimental Medicine* **215**:35-49 https://doi.org/10.1084/jem.20171868 | PubMed

Roukens M Guy, Peterson-Maduro Josi, Padberg Yvonne, Jeltsch Michael, Leppänen Veli Matti, Bos Frank L, Alitalo Kari, Schulte-Merker Stefan, Schulte Dörte (2015) Functional Dissection of the CCBE1 Protein: A Crucial Requirement for the Collagen Repeat Domain. *Circulation Research* **116**:1660-69 https://doi.org/10.1161/CIRCRESAHA.116.304949 | PubMed

Saharinen Pipsa, Eklund Lauri, Alitalo Kari (2017) Therapeutic Targeting of the Angiopoietin–TIE Pathway. *Nature Reviews Drug Discovery 2017 16:9* **16**:635-61 https://doi.org/10.1038/nrd.2016.278 | PubMed

Saharinen Pipsa, Kerkelä Katja, Ekman Niklas, Marron Marie, Brindle Nicholas, Lee Gyun Min, Augustin Hellmut, Koh Gou Young, Alitalo Kari (2005) Multiple Angiopoietin Recombinant Proteins Activate the Tie1 Receptor Tyrosine Kinase and Promote Its Interaction with Tie2. *The Journal of Cell Biology* **169**:239 https://doi.org/10.1083/JCB.200411105 | PubMed

Sato-Nishiuchi Ryoko, Doiguchi Masamichi, Morooka Nanami, Sekiguchi Kiyotoshi (2023) Polydom/SVEP1 Binds to Tie1 and Promotes Migration of Lymphatic Endothelial Cells. *Journal of Cell Biology* **222** https://doi.org/10.1083/JCB.202208047 | PubMed

Sato-Nishiuchi Ryoko, Nakano Itsuko, Ozawa Akio, Sato Yuya, Takeichi Makiko, Kiyozumi Daiji, Yamazaki Kiyoshi, Yasunaga Teruo, Futaki Sugiko, Sekiguchi Kiyotoshi (2012) Polydom/SVEP1 Is a Ligand for Integrin A9β1. *Journal of Biological Chemistry* **287**:25615-30 https://doi.org/10.1074/jbc.M112.355016 | PubMed

Savant Soniya, La Porta Silvia, Budnik Annika, Busch Katrin, Hu Junhao, Tisch Nathalie, Korn Claudia, et al. (2015) The Orphan Receptor Tie1 Controls Angiogenesis and Vascular Remodeling by Differentially Regulating Tie2 in Tip and Stalk Cells. *Cell Reports* **12**:1761 https://doi.org/10.1016/J.CELREP.2015.08.024 | PubMed

Seegar Tom CM, Eller Becca, Tzvetkova-Robev Dorothea, Kolev Momchil V, Henderson Scott C, Nikolov Dimitar B, Barton William A (2010) Tie1-Tie2 Interactions Mediate Functional Differences between Angiopoietin Ligands. *Molecular Cell* **37**:643-55 https://doi.org/10.1016/j.molcel.2010.02.007 | PubMed

Shen Bin, Shang Zhi, Wang Bo, Zhang Luqing, Zhou Fei, Li Taotao, Chu Man, et al. (2014) Genetic Dissection of Tie Pathway in Mouse Lymphatic Maturation and Valve Development. *Arteriosclerosis, Thrombosis, and Vascular Biology* **34**:1221-30 https://doi.org/10.1161/ATVBAHA.113.302923 | PubMed

Souma Tomokazu, Thomson Benjamin R, Heinen Stefan, Carota Isabel Anna, Yamaguchi Shinji, Onay Tuncer, Liu Pan, et al. (2018) Context-Dependent Functions of Angiopoietin 2 Are Determined by the Endothelial Phosphatase VEPTP. *Proceedings of the National Academy of Sciences of the United States of America* **115**:1298-1303 https://doi.org/10.1073/PNAS.1714446115 | PubMed

Wang Guangxia, Muhl Lars, Padberg Yvonne, Dupont Laura, Peterson-Maduro Josi, Stehling Martin, le Noble Ferdinand, et al. (2020) Specific Fibroblast Subpopulations and Neuronal Structures Provide Local Sources of Vegfc-Processing Components during Zebrafish Lymphangiogenesis. *Nature Communications* **11** https://doi.org/10.1038/s41467-020-16552-7 | PubMed

Young Terri L, Whisenhunt Kristina N, Jin Jing, LaMartina Sarah M, Martin Sean M, Souma Tomokazu, Limviphuvadh Vachiranee, et al. (2020) SVEP1 as a Genetic Modifier of TEK-Related Primary Congenital Glaucoma. *Investigative Ophthalmology and Visual Science* **61** https://doi.org/10.1167/IOVS.61.12.6 | PubMed

Yuan Hai Tao, Venkatesha Shivalingappa, Chan Barden, Deutsch Urban, Mammoto Tadanori, Sukhatme Vikas P, Woolf Adrian S, Ananth Karumanchi S (2007) Activation of the Orphan Endothelial Receptor Tie1 Modifies Tie2-mediated Intracellular Signaling and Cell Survival. *The FASEB Journal* **21**:3171-83 https://doi.org/10.1096/fj.07-8487com | PubMed

Peer reviews

Reviewer #1 (Public review):

Summary:

In this manuscript, Uphoff et al. propose a structural and mechanistic model in which the multidomain ECM protein SVEP1 enables Angiopoietin (ANG) binding to the orphan receptor TIE1, thereby promoting downstream receptor phosphorylation and signaling. Using AlphaFold-based modeling, the authors predict that the CCP20 domain of SVEP1 binds to TIE1, creating a composite surface that facilitates Angiopoietin association and TIE1 activation. The resulting ternary model (SVEP1-TIE1-ANG) offers a structural rationale for how SVEP1 converts TIE1 into a functional, ligand-responsive receptor. Additional models and biological assays suggest roles for other domains of SVEP1, such as CCP5-EGF-L7, although these interactions are predicted with low confidence. The authors interpret these findings as the first structural framework for how SVEP1 enables ANG-TIE1 signaling.

Strengths:

(1) The central hypothesis - that SVEP1 enables ANG binding to the orphan receptor TIE1 - is biologically compelling and addresses an important question in vascular biology.

(2) The AlphaFold-predicted ternary complex (SVEP1-TIE1-ANG) is plausible, high-confidence, and structurally consistent with prior functional data (e.g., poly-Ala scanning from Sato-Nishiuchi et al.).

(3) The authors' model offers a potential explanation for the previously observed role of SVEP1 in enhancing ANG signaling through TIE1 and may represent the first structural insight into TIE1's transition from orphan to ligand-activated receptor.

(4) The potential clinical implication - that a combinatorial ligand (ANG+SVEP1) can activate TIE1- could have translational relevance for vascular leak and inflammatory disease.

Comments on revised version:

The authors have adequately addressed my concerns.

https://doi.org/10.7554/eLife.106338.2.sa2

Reviewer #2 (Public review):

Uphoff and colleagues present the results of a study focused on characterizing the binding of SVEP1 to TIE1 along with Angiopoietin-2. Starting with computational prediction of SVEP1

binding to TIE1, the authors identify the region of SVEP1 that serves as a high-affinity ligand for TIE1. Advanced studies identify a weak secondary binding site within SVEP1 that appears to be sufficient but not necessary for its interaction with TIE1 based on in vivo rescue experiments. The most novel contribution of the manuscript seems to be the identification of angiopoietin-1 and -2 as co-factors that seem to enhance the binding of SVEP1 with TIE1 and impact downstream AKT signaling. They propose a complex in which SVEP1 binds to TIE1 and ANG2.

Although the first set of results is essentially confirmatory, the identification of ANG-2 as a "co-factor" enhancing the binding of SVEP1 to TIE1 and associated downstream signaling (i.e., Figures 3 and 4) is novel and is of interest. However, the manuscript and its conclusions would greatly benefit from some clarifying details and additional experiments to ensure rigor and support specific claims.

Comments on revised version:

I have no further comments. The authors have addressed my concerns.

https://doi.org/10.7554/eLife.106338.2.sa1

Author response:

The following is the authors' response to the original reviews.

> ***Public Reviews:***
>
> ***Reviewer #1 (Public review):***
>
> *Summary:*
>
> *In this manuscript, Uphoff et al. propose a structural and mechanistic model in which the multidomain ECM protein SVEP1 enables Angiopoietin (ANG) binding to the orphan receptor TIE1, thereby promoting downstream receptor phosphorylation and signaling. Using AlphaFold-based modeling, the authors predict that the CCP20 domain of SVEP1 binds to TIE1, creating a composite surface that facilitates Angiopoietin association and TIE1 activation. The resulting ternary model (SVEP1-TIE1-ANG) offers a structural rationale for how SVEP1 converts TIE1 into a functional, ligand responsive receptor. Additional models and biological assays suggest roles for other domains of SVEP1, such as CCP5-EGF-L7, although these interactions are predicted with low confidence. The authors interpret these findings as the first structural framework for how SVEP1 enables ANG-TIE1 signaling.*
>
> *Strengths:*
>
> *(1) The central hypothesis - that SVEP1 enables ANG binding to the orphan receptor TIE1 - is biologically compelling and addresses an important question in vascular biology.*
>
> *(2) The AlphaFold-predicted ternary complex (SVEP1-TIE1-ANG) is plausible, high-confidence, and structurally consistent with prior functional data (e.g., poly-Ala scanning from Sato-Nishiuchi et al.).*
>
> *(3) The authors' model offers a potential explanation for the previously observed role of SVEP1 in enhancing ANG signaling through TIE1, and may represent the first structural insight into TIE1's transition from orphan to ligand-activated receptor.*
>
> *(4) The potential clinical implication - that a combinatorial ligand (ANG+SVEP1) can activate TIE1- could have translational relevance for vascular leak and inflammatory disease.*

> *Weaknesses:*
>
> *(1) Lack of structural validation and mechanistic follow-up: Despite the promising AlphaFold model, there are no figures of the predicted interface, no residue-level interactions shown, no ipTM values reported, and no experimental follow-up to test the interface. PAE plots are incorrectly used as confidence justifications, which is not appropriate for complex predictions.*

We have appended the data showing AlphaFold-predicted interfaces, including residues, hydrogen bonds, and surface complementarity. We also added ipTM scores and confidence plots for the predicted complexes.

> *(2) Biophysical validation is missing: No surface plasmon resonance (SPR), ITC, or biochemical assays are included to confirm ternary complex formation or quantify binding kinetics. Given the manuscript's structural focus, this is a major gap. For instance, an SPR experiment where ANG is immobilized, and TIE1 binding is measured {plus minus} SVEP1, would directly test the model. And allow direct comparison to ANG-TIE2.*

We have addressed this question and performed ELISA assays to measure binding affinities between SVEP1 and TIE1 in presence or absence of ANG1 or ANG2, thus confirming that the affinity is increased in the presence of ANG1 or ANG2.

> *(3) Missed opportunity for mutagenesis-driven validation: The manuscript does not include any interface-targeted mutations, despite clear opportunities. For example, mutating T2595 in SVEP1 (to R) or mutating the TIE1-specific residues (residues PL 202-203 to LF) could strongly test the model and potentially reveal dominant-negative behaviors. E.g. A T2595 mutant should block ANG binding but not TIE1 binding.*

We have depicted figures of the interfaces including P202-L203 and included the TIE1 P202L L203F mutant, as well as the previously described SVEP1 (E2568A - G2569A) mutant in our experimental data. The T2595 mutant was not included in the current study, for the following reason: Modeling suggested that replacing T2595 with an Arg will cause steric and charge clashing with 469GKL471 of ANG1 and 467NKFN470 of ANG2, thus reducing its binding to ANG2 although T2595 does not interact with ANG1/2. A SVEP1 protein comprising CCP15 to the C-terminus with the T2594R mutation shows reduced binding to ANG2, but also reduced binding to TIE1. As the mutation hinders interaction with both TIE1 and ANG2, the data is not included in the manuscript.

> *(4) Overinterpretation of weak models: The additional AlphaFold model involving the CCP5-EGFL7 domains binding TIE1 has extremely low confidence (ipTM < 0.15) when reexamined by this reader and should not be emphasized. There is no biophysical evidence or binding data (SPR) to support this interaction, and its inclusion detracts from the much stronger CCP20 model.*

We agree with this point made by both reviewers and have removed the data on CCP5-EGFL7 from the manuscript.

> *(5) Language around modeling is overstated and potentially misleading: Terms like "unequivocal," "high-affinity," or "affirms strong binding" in reference to AlphaFold predictions are inappropriate. These are hypotheses -not confirmations - and must be tested at the biochemical level. This should be clarified throughout the manuscript to ensure non-experts do not misinterpret modeling confidence as binding affinity.*

We agree with the reviewer, and have adjusted the wording.

> *(6) Negative stain EM data is not informative due to low resolution and lack of defined interfaces; unless replaced by higher-resolution Cryo-EM, this should be omitted. Better would be co-gel filtration, AUC, or SEC-MALLs with ANG-SVEP1-TIE1.*

We have now appended the data by adding gold-labelled TIE/ANG proteins, thus enhancing clarity.

> *(7) Disjointed narrative: The manuscript presents a compelling mechanism involving CCP20-driven ANG binding to TIE1, but then becomes fragmented by introducing the low-confidence CCP5-EGFL7 model and speculative higher-order polymerization models that are not experimentally supported.*

We agree with this point and have have centered the manuscript around CCP20. We removed data concerning CCP5-EGFL7 as suggested by both reviewers.

> ***Reviewer #2 (Public review):***
>
> *Uphoff and colleagues present the results of a study focused on characterizing the binding of SVEP1 to TIE1 along with Angiopoietin-2. Starting with computational prediction of SVEP1 binding to TIE1, the authors identify the region of SVEP1 that serves as a high-affinity ligand for TIE1. Advanced studies identify a weak secondary binding site within SVEP1 that appears to be sufficient but not necessary for its interaction with TIE1 based on in vivo rescue experiments. The most novel contribution of the manuscript seems to be the identification of angiopoietin-1 and -2 as co-factors that seem to enhance the binding of SVEP1 with TIE1 and impact downstream AKT signaling. They propose a complex in which SVEP1 binds to TIE1 and ANG2.*
>
> *Although the first set of results is essentially confirmatory, the identification of ANG-2 as a "cofactor" enhancing the binding of SVEP1 to TIE1 and associated downstream signaling (i.e., Figures 3 and 4) is novel and is of interest. However, the manuscript and its conclusions would greatly benefit from some clarifying details and additional experiments to ensure rigor and support specific claims.*

We have addressed the reviewers concerns and significantly appended the manuscript. Most importantly, we provide structural validation of AlphaFold models reporting interfaces, residue-level interactions and ipTM values. We have included new biophysical validation of binding kinetics of SVEP1 and TIE1 in the presence or absence of ANG1 or ANG2. Furthermore, we have removed the data on CCP5-EGFL7 from the manuscript in order to retain focus on the CCP20 domain.

> ***Recommendations for the authors:***
>
> ***Reviewer #1 (Recommendations for the authors):***
>
> *The AlphaFold modeling for the CCP20-based interactions is strong (as determined by this reader rerunning and getting ipTM values and visually inspecting the interactions "because this is not in the manuscript"). As presented, the manuscript stops at the hypothesis-generation stage. Validation is needed to fulfill the paper's title and claims. The structure-function link is not demonstrated, despite an obvious and achievable experimental path (mutagenesis, SPR, kinetics).*
>
> *Additional Context and Suggestions*
>
> *(1) Show and label AlphaFold-predicted interfaces, including residues, hydrogen bonds, and surface complementarity.*

We have appended the data in the new supplementary figures 1.1, 1.2, 2.1 and 2.2

> *(2) Provide ipTM scores and confidence plots for each predicted complex.*

We have added the values and plots in the new supplementary figures.

> *(3) Perform SPR assays with ANG-coated surfaces and measure binding of TIE1 {plus minus} SVEP1. Compare to TIE2 binding for context.*

We performed the proposed experiment using an ELISA assay to measure binding affinities between SVEP-1 and TIE1 in presence or absence of ANG2 and included these data in the manuscript in figure 2.

> *(4) Test interface mutants: e.g., T2595R in SVEP1 (should impair ANG recruitment but not TIE1 binding), or PL→LF muta on in TIE1 (should disrupt SVEP1 binding).*

We have depicted figures of the interfaces including P202-L203 and included the TIEP202L L203F mutant, as well as the previously described SVEP1 (E2568A - G2569A) mutant in our experimental data. The T2595 mutant was not included in the current study. Our modeling suggested that replacing T2595 with an Arg will cause steric and charge clashing with 469GKL471 of ANG1 and 467NKFN470 of ANG2 thus reduce its binding to ANG2 although T2595 does not interact with ANG1/2. A SVEP1 protein comprising CCP15 to the C-terminus with the T2594R mutation shows reduced binding to ANG2, but also reduced binding to TIE1. As the mutation hinders interaction with both, TIE1 and ANG2, the data is not included in the manuscript.

> *(5) Clarify in the Introduction that SVEP1 is a large, multidomain ECM protein to help readers contextualize the domain names early on. Do not use terms like CCP before defining them.*

We added: “Svep1 encodes a 3571 amino acid long extracellular matrix protein containing different domains such as Willebrand factor type A domain (vWF), ephrin-receptor like domains, complex control protein (CCP) domains, and Hyalin repeats at the N-terminus. The C-terminus mainly consists of CCP and EGF domains. Svep1 is expressed in mesenchymal cells, but not in endothelial cells, and functions non-cell-autonomously (Karpanen et al. 2017; Morooka et al. 2017)”.

> *(6) Replace or remove negative-stain EM unless higher-resolution cryo-EM data are available.*

We would like to retain the EM data, but have now replaced the negative-stain EM by adding gold-labelled TIE/ANG Proteins to verify that the proteins we show are the ones we expect. The reason we would like to retain the data is that TIE1 has been considered for so many years as an orphan receptor, and thus we consider it appropriate to demonstrate SVEP1/TIE1 binding using multiple methods.

> *(7) Reframe claims around modeling to avoid overstatement. For example: "The model suggests a plausible mechanism consistent with prior biochemical data" is more appropriate than "unequivocal".*

We agree with the reviewer, and have adjusted the wording.

> *(8) Consider narrowing the focus: the CCP20-TIE1-ANG model is a strong story on its own. The CCP5EGFL7 model and polymerization hypotheses are not essential and may dilute the impact.*

Since this point was made by more than one reviewer, we have removed the data on CCP5EGFL7 from the manuscript.

> *(9) Properly define TIE1: Tyrosine kinase with Ig and EGF domains.*

We have corrected the full protein name for TIE1 and added: “TIE1 and Tie2 exhibit a high degree of homology with a globular head domain consisting of three immunoglobulin-like (Ig) domains and three epidermal growth factor-like (EGF) modules and a short stalk formed by three fibronectin type III repeats, while the N-terminal two Ig domains of Tie2 harbor the angiopoietin binding site (Macdonald et al. 2006).” We also added: “D1 and D2 refer to the two N-terminal Ig domains, D3 refers to the three EGF domains and D4 to the third Ig domain of TIE1 or TIE2.”

> *(10) Use RTK, not tyrosine kinase receptors TKR.*

Tyrosine Kinase receptor was replaced by receptor tyrosine kinases (RTKs)

> *(11) PDBs (.cif and .json files) of the models must be supplied for the readers so they don't need to rerun the AlphaFold jobs.*

We are providing all PDBs with the revised manuscript.

> ***Reviewer #2 (Recommendations for the authors):***
>
> *Major comments:*
>
> *(1) In several locations, the authors state that alphafold detects an "unequivocal" and/or "high affinity" interaction. Experts on computational structure prediction can weigh in, but I am not sure it is accurate to say that alphafold predicts affinity. Quantitative estimates of the prediction confidence or other parameters of the alphafold output are not provided.*

Thank you for the comment, we agree with the reviewer and have adjusted the wording. We have also appended the data showing interfaces, ipTM scores and confidence plots for the predicted complexes.

> *(2) In Figure 1C, what concentrations of TIE1 and TIE2 are being used in the SPR experiments shown?*

We have added the concentrations of the proteins to the methods section

> *(3) In Figure 1C, what is the affinity constant (KD) of the interaction between SVEP1 and TIE1 and SVEP1 and TIE2?*

We have added the values of affinity constants to the manuscript text.

> *(4) In Figure 1C, the authors immobilize a "70kD" fragment of human SVEP1 to determine the interaction between SVEP1 and TIE1. How does the affinity they measure between the SVEP1 fragment and TIE1 compare to the affinity between immobilized full-length SVEP1 with TIE1?*

The largest molecule we used in any assay is not full-length SVEP1, but consisted of a C-terminal SVEP1 protein spanning from the first EGF domain to the C-terminus (approximately 295 kDa) as previous studies have shown that SVEP1 is proteolytically cleaved N-terminal to the first EGF domain, generating a protein of this size. In our ELISA assays, this molecule has a higher affinity to TIE1 than the 70 kD fragment. We have included data for the 70 kDa as well as for the 295 kDa fragment in the manuscript. ELISA assays have used larger SVEP1 fragments (as indicated in the figure legends), the SPR assay was performed with the 70 kDa fragment.

> *(5) How does the alphafold structure prediction for the "70kD" fragment of hSVEP1 compare to the prediction of the same 70kD fragment from the full-length protein prediction?*

All modellings using different SVEP1 fragments including the 70 kD and full-length version identify the putative binding site at position CCP20. While AlphaFold3 can predict the correct domain folds in both the 70kDa fragment and full-length SVEP1, the orientation of these domains is highly variable due to flexible linkers between each domain module. This flexibility effects the output confidence metrics, thereby hampering our interpretation of the models. Therefore, we conducted the structural prediction of the complexes with smaller fragments and not the full-length SVEP1.

> *(6) What are the amino acids for the 70kD fragment?*

The relevant amino acids are 2261-2890. The accession number and amino acids of each protein have been listed in the key resources table.

> *(7) In Figure 1D, what is being depicted by the red stars? This is not explained in the text or figure legend.*

We have replaced figure 1D.

> *(8) By itself, Figure 1D is not terribly informative and in my opinion does not support the statement that the authors "were able to directly visulalize the attachment of SVEP1 and TIE1." As a minimum, the authors should repeat the same set of images with SVEP1 and TIE2, but other approaches, such as labeling, could be performed.*

We replaced figure 1D with new data and gold-coated protein enhancing clarity. We think it beneficial to demonstrate SVEP1/TIE1 binding using multiple methods as TIE1 has been considered as an orphan receptor for so many years. We have not performed these experiments with TIE2 proteins as we were not able to show binding of TIE2 to SVEP1 with other assays.

> *(9) What is being stained in Figure 1D? Full-length SVEP1/TIE1? Or fragments of these proteins?*

We replaced figure 1D by a new assay with labeled proteins using the 150 kDa version of SVEP1 and the ectodomain of TIE1 as well as ANG1 or ANG2 (new figure 1D and new supplementary figure 2.3). TIE1/ANG proteins were gold-labelled. The protein fragments used in this assay are described in detail in the methods section.

> *(10) The authors discover CCP6-EGFL7 as a low-affinity binding region of SVEP1 for TIE1. Is this region in physical proximity to CCP20 (the high-affinity binding region for TIE1) based on alphafold prediction? How would the authors think this is binding TIE1?*

We have removed this data set (see comment to reviewer 1's request).

> *(11) What is the affinity constant (KD) for CCP6-EGFL7 with TIE1?*

We have removed this data set (see comment to reviewer's 1 request).

> *(12) The authors claim that ANG1/ANG2 increase affinity between SVEP1 and TIE1 based on immunoblotting. Immunoblots are semi-quantitative at best. If the claim is higher affinity, I think the authors should measure this by SPR and determine the KD between immobilized SVEP1 with TIE1 in the absence and presence of ANG1 and/or ANG2.*

We conducted ELISA assays (figure 2) showing that the affinity is increased in the presence of ANG1 or ANG2 and agree with this reviewer that this strengthens the data.

> *(13) In Figure 3, can the authors explain why ANG1/2 does not pull down with SVEP1/TIE1?*

We noticed that upon transfection of TIE1 into HEK cells, ANG1/2 is almost undetectable anymore in the total lysate. Thus, we believe that after the pull down we are below the detection limit.

> *(14) In Figure 3, what is "TL"? I assume total lysate, but this is not specified.*

Thank you, we now specify TL as total lysate.

> *(15) In Figure 3 "TL" panel (again, I assume this is total lysate), why are the ANG1/2 immunoblots so weak when co-transfected with TIE1?*

We consider it likely that in the presence of TIE1, ANG1/2 proteins are internalized and digested. Another reason for low signals could be that upon transfection of two plasmids, the amount of ANG1/2 protein is reduced as the cell has limited capacity for transcription and translation.

> *(16) In Figure 3B, why is the SVEP1 fragment now 150kD when 70kD fragment was previously used? What domains are contained in this 150kD fragment?*

We now better define the domains of the 150kD SVEP1 fragment. The 150 kD fragment was the one produced first and available in high amounts in our laboratory and thus used for functional assays. The 70 kDa fragment together with ANG2 also induces phosphorylation of AKT, but it was not used in as many conditions/replicates as the amounts we had available were lower.

> *(17) In Figure 4A, signaling with SVEP1 by itself and ANG2 by itself should be shown to support the claims being made.*

We added the lines for SVEP1 and ANG2, and also the quantification. SVEP1 itself already affects the phosphorylation of TIE1, most likely because hdLECs produce ANG2 by themselves. We show this with the ANG2 blocking antibody for pAKT.

> *(18) For pAKT, what are the concentations of proteins being used and the times of incubation?*

This information is provided in the Materials and Methods section. We added the concentration of the anti-ANG2 antibody, which was missing.

> *(19) It seems that p-AKT and AKT are being blotted on different gels. If this is correct, loading controls need to be shown for p-AKT blot.*

We added HSC70 as a loading control for both blots.

> *(20) It is interesting that anti-ANG2 antibody inhibits SVEP1-induced p-AKT signaling. As the authors may know, SVEP1 has been identified as a receptor for PEAR1, which also leads to downstream p-AKT signaling, which seems to be independent of ANG2. Do the LECs being used here express PEAR1? If these cells express PEAR1, how do the authors think ANG2 silencing will eliminate SVEP1-associated p-AKT signaling?*

hdLECs express PEAR1. However, we show that p-AKT signaling is attenuated after siRNA KO of TIE1. Thus, the downstream signaling is dependent on TIE1 (Figure3).

> *(21) Again, experts on computational structure prediction can weigh in, but I am not sure how to interpret the prediction of the 2:2:2 stoichiometry for the theoretical SVEP1/TIE1/ANG1-2 complex. Are there quantitative estimates of the confidence that can*

> *be provided? Did the authors attempt to model this complex with different stoichiometries? It is difficult to know how relevant this model is without any experimental results supporting this result.*

Since 1:1:1 is the smallest possible triple complex, it is our starting point. We can model a 2:2:2 version, but anything larger than this AlphaFold will not run. Furthermore, we now provide quantitative estimates of confidence with the pLDDT, PAE, pTM, ipTM scores for all models including the 2:2:2 complexes.

> *Minor comments:*
>
> *(1) The authors could consider including a reference to alphafold on line 102.*

We have added a reference for AlphaFold2 and 3

> *(2) The authors should refer to surface plasmon resonance (SPR) assays by this term as opposed to using the brand name Biacore.*

We agree with the reviewer and have changed the term Biacore to SPR.

https://doi.org/10.7554/eLife.106338.2.sa0